

journal homepage: [www.elsevier.com/locate/csbj](http://www.elsevier.com/locate/csbj)

# ADP-ribosylation systems in bacteria and viruses

Petra Mikočević<sup>a,1</sup>, Andrea Hloušek-Kasun<sup>a,1</sup>, Ivan Ahel<sup>b,\*</sup>, Andreja Mikoč<sup>a,\*</sup>

<sup>a</sup> Division of Molecular Biology, Ruđer Bošković Institute, Zagreb, Croatia

<sup>b</sup> Sir William Dunn School of Pathology, University of Oxford, UK



## ARTICLE INFO

### Article history:

Received 1 February 2021

Received in revised form 7 April 2021

Accepted 7 April 2021

Available online 17 April 2021

### Keywords:

ADP-ribosylation  
ADP-ribosyl transferase  
ADP-ribosyl hydrolase  
PARP, PARG  
Macrodomain  
Toxin-antitoxin system

## ABSTRACT

ADP-ribosylation is an ancient posttranslational modification present in all kingdoms of life. The system likely originated in bacteria where it functions in inter- and intra-species conflict, stress response and pathogenicity. It was repeatedly adopted via lateral transfer by eukaryotes, including humans, where it has a pivotal role in epigenetics, DNA-damage repair, apoptosis, and other crucial pathways including the immune response to pathogenic bacteria and viruses. In other words, the same ammunition used by pathogens is adapted by eukaryotes to fight back. While we know quite a lot about the eukaryotic system, expanding rather patchy knowledge on bacterial and viral ADP-ribosylation would give us not only a better understanding of the system as a whole but a fighting advantage in this constant arms race. By writing this review we hope to put into focus the available information and give a perspective on how this system works and can be exploited in the search for therapeutic targets in the future. The relevance of the subject is especially highlighted by the current situation of being amid the world pandemic caused by a virus harbouring and dependent on a representative of such a system.

© 2021 The Author(s). Published by Elsevier B.V. on behalf of Research Network of Computational and Structural Biotechnology. This is an open access article under the CC BY-NC-ND license (<http://creativecommons.org/licenses/by-nc-nd/4.0/>).

## Contents

1. Introduction	2367
2. ADP-ribosyl transferases	2367
2.1. Diphtheria toxin family ARTs	2370
2.1.1. Diphtheria and diphtheria-like toxins	2370
2.1.2. Bacterial PARPs	2373
2.1.3. Rifampin ARTs	2373
2.2. Cholera toxin family ARTs	2373
2.2.1. Cholera and cholera-like toxins	2373
2.2.2. Pierisins	2374
2.2.3. Viral ARTs	2374
2.3. Divergent ARTs	2374
2.3.1. Tpt1/KptA and CC0527 ARTs	2374
2.3.2. Gb/RolB ART	2375
3. Sirtuins	2375
4. ADP-ribosyl hydrolases	2376
4.1. Macrodomain family ARHs	2376
4.1.1. Bacterial MacroD-like ARHs	2376
4.1.2. Viral MacroD-like ARHs	2377
4.1.3. Bacterial TARG1-like ARHs	2377
4.1.4. Bacterial PARGs	2377
4.2. DraG-like family ARHs	2378

\* Corresponding authors.

E-mail addresses: [ivan.ahel@path.ox.ac.uk](mailto:ivan.ahel@path.ox.ac.uk) (I. Ahel), [mikoc@irb.hr](mailto:mikoc@irb.hr) (A. Mikoč).

<sup>1</sup> These authors contributed equally to this work.

<https://doi.org/10.1016/j.csbj.2021.04.023>

2001-0370/© 2021 The Author(s). Published by Elsevier B.V. on behalf of Research Network of Computational and Structural Biotechnology.

This is an open access article under the CC BY-NC-ND license (<http://creativecommons.org/licenses/by-nc-nd/4.0/>).

5. Reversible ADP-ribosylation systems	2378
5.1. DraT/DraG	2378
5.2. DarT/DarG	2378
5.3. SirTM	2379
5.4. ParT/ParS	2379
5.5. SidE/SidJ/DupA	2379
5.6. Tre1/Tri1	2379
6. Conclusions	2380
CRedit authorship contribution statement	2380
Declaration of Competing Interest	2380
Acknowledgements	2380
References	2380

## 1. Introduction

Post-translational modifications (PTMs) introduce enormous versatility to the genome-encoded proteome. By altering localization, activity, stability and interaction partners of proteins it provides means to multitask even a more restricted menu of proteins (bacteria code for an average of 3200, viruses for around 42 proteins; in comparison to more than 15 000 in eukaryotes) [1]. The human ADP-ribosylation system has been the focus of most studies, but it is becoming obvious that bacterial and viral repertoire does not fall short of diversity and candidates, that could also be targeted for therapeutic purposes. On a physiological level, it enables microorganisms (and viruses) to adapt to the changes in their environment - be it a difference in availability of resources, presence of intra- and interspecies toxins, or used as a weapon that neutralizes the host defences or simply hijacks the host's resources.

The ADP-ribosylation PTM entails the transfer of one or more interlinked molecules of ADP-ribose (ADPr) moieties from redox cofactor  $\beta$ -nicotinamide adenine dinucleotide ( $\text{NAD}^+$ ) onto nucleic and amino acid side chains with nucleophilic oxygen, nitrogen, or sulphur, resulting in O-, N-, or S-glycosidic linkage to the ribose, and a phosphodiester bond with O- on aspartate and glutamate or small molecules such as antibiotics (Fig. 1). The system consists of ADP-ribosyl transferases (ARTs) that covalently attach the ADPr onto targets and the ADP-ribosyl hydrolases (ARHs) which cleave off the ADPr. The majority of ARTs catalyse the transfer of a single ADPr onto the target. Only a few members of the poly-ADPr polymerase (PARP) family can synthesize long chains of poly-ADPr (PAR). For conciseness, we will call the mono-ADP-ribosylation - MARYlation and the addition of poly-ADPr - PARYlation. Based on the chemical nature, length and complexity of the ADPr-target bond, different enzymes are needed to reverse it. The hydrolysis of the ADPr from the target is achieved by two evolutionarily and structurally distinct protein families of ARHs - the macrodomain and the DraG-like hydrolases.

Proteins involved in the ADP-ribosylation cycle are unevenly distributed among bacteria, with ARHs being more abundant than ARTs. There are bacterial species limited to very few ART or ARH homologues or just one of the specialized reversible systems (e.g. pathogenic bacteria). On the other hand, there are bacteria with a complete repertoire of ART/ARH homologues that can use ADP-ribosylation in its entirety (Table 3).

Based on the available data and phylogenetic analysis, the ADP-ribosylation has emerged as a part of the bacterial conflict/stress-response system and was taken up by the eukaryotes from the last universal common ancestor. There are indications that it was also later exchanged in both directions via lateral transfer [2–4]. Part of the reason for this constant exchange and evolution is the selective pressure between the pathogenic bacteria and viruses versus host

immune system, both utilizing ADP-ribosylation enzymes as ammunition. The typical pathogenic bacterial ARTs act as toxins and numerous viruses manipulate host PTM machinery, to regulate their replication or evade host immunity response. It is thought that both the pathogens and the eukaryotic host innate immune system often obtain compensatory mutations to gain the advantage in this constant arms race [5–8].

Still, ADP-ribosylation in bacteria fulfils important endogenous functions which are still poorly understood. Some examples come from studying sporulation in *Bacillus subtilis* [9], development and cell-cell interaction in *Myxococcus xanthus* [10–12], but best evidence comes from *Streptomyces* species [13–16]. *Streptomyces* are soil-dwelling Gram-positive bacteria that are best known for their large genome (*S. coelicolor* codes for almost 8000 proteins [17]) and a complex life cycle that includes morphological differentiation and the production of various secondary metabolites including antibiotics, anti-cancer drugs and immunosuppressors. Over the last 30 years, ADP-ribosylation was found to be involved in growth, differentiation and secondary metabolite production in *S. griseus* and *S. coelicolor* [13–14,16,18–21]. *S. coelicolor* possesses enzymes from essentially each ADP-ribosylation metabolism family (Tables 1, 2 and 3) and are therefore an appropriate system to study the breadth of the bacterial ADP-ribosylation system.

Many excellent reviews about the ADP-ribosylation systems have been written [2–3,12,6–8,22–27], but a comprehensive overview of the ART/ARH system with a focus on bacteria and viruses is long overdue. In the course of this review, we will analyse each group and try to shine some light on their particularities based on the structural, biochemical and functional data available.























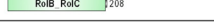


## 2. ADP-ribosyl transferases

The ART superfamily can be divided into two major structurally and functionally different families based on their founder transferase: the Diphtheria toxin (DTX) and the Cholera toxin (CTX) family [2,22,28]. We will also discuss a group of structurally unrelated  $\text{NAD}^+$ -dependent deacetylase with some members showing robust ART activity - sirtuins [29] (Table 1).

Despite the primary sequence diversification, the ARTs share a common structural organization pattern: an N-terminal portion (with highly conserved histidine in DTX, or arginine in CTX) responsible for  $\text{NAD}^+$ -binding; and a C-terminal portion with a highly acidic region with a conserved glutamate residue crucial for the cleavage of  $\text{NAD}^+$  via the  $\text{S}_{\text{N}}1$  reaction mechanism. Mutation of this key glutamate residue results in a several hundred-fold loss of ART activity and cytotoxicity [22,30]. The common 3D core is formed by six strands, most of which are followed by a downstream helical element [2]. The  $\text{NAD}^+$  binds to the hydrophobic cleft formed within the core (Fig. 3). Most of the ARTs have three


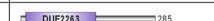







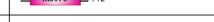



**Table 1**  
Bacterial and viral ARTs.

ART	Bacterium/virus	PDB/UniProt	Domain architecture	Motif/catalytic aa	Target	Effect/function	Ref.
Diphtheria toxin (DTX) family							
DTX	<i>Corynebacterium diphtheriae</i>	1DDT, 1DTP, 1MDT, 1FOL, 1TOX, 1SGK, 1XDT, 7K7B-E		H-Y-E (H24, Y65, E148)	EF2 (Dipthamide 715 -NH-)	Inhibition of translation	42
PARP	<i>Herpetosiphon aurantiacus</i>	A9B244		H-Y-E	unknown	unknown	4
	<i>Clostridioides difficile</i> CD160	T3DQ72					50
	<i>Mycobacteroides abscessus</i>	A0A1N3ZHFO					
	<i>Butyrivibrio proteoclasticus</i>	E0S444					
Arr	<i>Mycobacterium smegmatis</i>	2HW2		H-Y-D (H19, Y49, D84)	Rifampin (C23-OH)	Rifampin inactivation	38
SCO2860	<i>Streptomyces coelicolor</i>	Q9RD91		H-Y-D			
Cholera toxin (CTX) family							
CTX	<i>Vibrio cholerae</i>	1S5B-F, 1XTC, 2A5D, 2A5F, 2A5G		R-S-E (R7, S61, E110, E112)	Gsa (R201)	Adenylate cyclase activation	74
Scabin	<i>Streptomyces scabiei</i>	5DAZ, 5EWY, 5EWK, 6VPA, 6APY, 5UVQ, 5TLB		R-S-E (R77, S117, W155, Q158, E160)	DNA (G-N2)	Virulence factor?	86, 87, 199
SCOS461	<i>Streptomyces coelicolor</i>	5ZJ4, 5ZJ5		R-S-E (R81, S121, W159, Q162, E164)	DNA (G-N2), tRNA	Regulation of morphological differentiation and antibiotic production	15, 63, 89
MTX	<i>Lysinibacillus sphaericus</i>	2CB4, 2CB6, 2VSA, 2VSE		R-S-E (R97, S142, E195, E197)	EF-Tu (R)	Inhibition of protein synthesis	65, 84, 90, 200
Alt	<i>Escherichia virus T4</i>	P12726		R-S-E	soRNA polymerase (R265), MazF (R84)	Preferential expression of viral genes; fighting antiphage defence	91, 92
ModA	<i>Escherichia virus T4</i>	P39421		R-S-E (R72, S109, F127, F129, E165)	soRNA polymerase (R265)	Preferential expression of viral genes	93
Tre1	<i>Serratia proteamaculans</i>	6DRH		R-S-E	FtsZ (R174), EF-Tu, RNase E, LolD	Interbacterial defence system	197
DraT	<i>Rhodospirillum rubrum</i>	Q2RVN5		R-S-E	Nitrogenase reductase (R101)	Inhibition of nitrogenase reductase	176
SdeA	<i>Legionella pneumophila</i>	5YSI, 5YSJ, 5YSK		R-S-E (E860, E862)	Ubiquitin (R42)	Blocking of ubiquitin signalling	184, 194, 201
Divergent ARTs							
Tpt1	<i>Clostridium thermocellum</i>	6E3A, 6EDE		H-H-h (R18, H19, R68, R121)	5'P-RNA, 5'P-DNA	unknown	99, 103
SCO3953	<i>Streptomyces coelicolor</i>	Q9ZBX9			5'P-RNA		98
CC0527	<i>Caulobacter crescentus</i>	2O0Q, 2O0Q, 2O0P, 2JQN		E160	Antibiotic?	Antibiotic inactivation?	2
DarT	<i>Thermus aquaticus</i>	B7A853			ssDNA (T)	DNA damage	179, 180
ParT	<i>Sphingobium sp.</i>	6DOH, 6DOI		R-Y-N (R31, E52, H56)	Prs (K182, S202)	Interfering with nucleotide biosynthesis	183
AcrIF11	<i>Pseudomonas aeruginosa</i> PA14	6KYF		H-H-D (D115)	Cas8f (N250)	Inactivation of CRISPR system	95
6b	<i>Rhizobium radiobacter</i>	3AQ3		Y-T-Y-Y (Y66, T93, Y121, Y153)	Histone H3, SE, AGO1	Disturbance of miRNA pathway	108
Sirtuin family							
TmSir2	<i>Thermotoga maritima</i>	2H4F, 2H4H, 2H4J, 2HS9, 3D4B, 3D81		HG (H116)	Acetyl-p53 (K, R)	unknown	29, 117
SirTM	<i>Streptococcus pyogenes</i>	5A3A, 5A3B, 5A3C		QG-R (N118, Q137, R192)	GcvH-L (D27)	Regulation of oxidative stress response	112

ND stands for a non-defined domain.

**Table 2**  
Bacterial and viral ARHs.

ARH	Bacterium/virus	PDB/UniProt	Domain architecture	Motif/catalytic aa	Target	Effect/Function	Ref.
<b>Macrodomain family</b>							
PARG	<i>Thermomonaspara curvata</i>	3SIG-J		GGGX <sub>6</sub> QEE (E114, E115, F227)	Protein-PAR (exo-activity)	unknown	4
PARG	<i>Deinococcus radiodurans</i>	5ZDA-F		GGGX <sub>6</sub> QEE (E112)	Protein-PAR (endo- and exo-activity)	DNA damage response	51
YmdB	<i>Escherichia coli</i>	5CB3, 5CB5, 5CMS		N-GGVD-GVYG (N22, N25, G32, D35, H39, Y126)	OAADPr, protein-ADPr	Regulation of RNase III activity and biofilm formation	130,135-137
OiMacroD	<i>Oceanobacillus iheyensis</i>	5FUD, 5L9K, 5L9Q, 5LAU, 5LBP, 5LCC		N-GGVD-GVYG (N30, G37, D40, Y134)	OAADPr, protein-ADPr	unknown	128
SCO6450	<i>Streptomyces coelicolor</i>	Q9ZBG3		N-GGVD-GVY	Protein-ADPr, ADPr-5'P-dsDNA, dsDNA-3'P-ADPr, ADPr-5'P-RNA	unknown	98, 138
Nsp3	SARS-CoV-2	6WEN, 6VXS, 6W02, 6W0J, 6WEY, 6Z72, 6Z6I, 6Z5T, 6W6Y, 6WCF, 6YWK, 6YWL, 6YWM		N-GGV-GIFG (N40, G48, G130, F132)	Protein-ADPr	Promotion of virus replication and suppression of the antiviral response	7, 134, 146, 150, 151
FmTARG1	<i>Fusobacterium mortiferum</i>	C3WDV1		TK-G-G-D	OAADPr, protein-ADPr, protein-PAR	unknown	154
DarG	<i>Thermus aquaticus</i>	5M31, 5M3E		TK-G-G (K80)	ssDNA-T-ADPr	Antitoxin	179-181
SCO6735	<i>Streptomyces coelicolor</i>	5E3B		not fully explained	Protein-ADPr	Regulation of antibiotic production	21
<b>DraG-like family</b>							
DraG	<i>Rhodospirillum rubrum</i>	2WOC, 2WOD, 2WOE		E-D-D (+ Mn) (E28, D60, D97)	Protein-R-ADPr	Regulation of nitrogen fixation	171
Tri1	<i>Serratia proteamaculans</i>	6DRE		E-D-D	Protein-R-ADPr	Antitoxin	197

**Table 3**  
Distribution of ART and ARH homologues in different bacterial species.

Bacterium	PARP	Tpt1	Arr	DUF952	Other ARTs	PARG	MacroD	TARG1	ARH (DraG-like)	DarT/DarG	SirTM	ParT/ParS	Tre1/Tri1
<i>Caulobacter crescentus</i> CB15				Q9AAR9									
* <i>Rhizobium radiobacter</i>		A0A1B9T2R3		A0A4D7XT44	A0A1B9UDL6 (6b)			A0A2L2LMG0 A0A4Z1Q3G1	A0A546Y2U9				
<i>Rhodospirillum rubrum</i> ATCC 11170				Q2RX28	Q2RVN5 Q2RUK5 (DraTs)				Q2RVN6				
<i>Sphingobium</i> sp. (str. YBL2)				A0A0C5X7U0								A0A0C5XL88 A0A0C5XKJ0	
* <i>Escherichia coli</i> O127:H6 (str. E2348/69)		B7UQW9					B7UP60		B7UF66	B7UP20 B7UP19			
* <i>Legionella pneumophila</i> subsp. <i>pneumophila</i> ATCC 33152					Q5ZTK4 (SdeA)								
<i>Serratia proteamaculans</i> 568													A8GG78 A8GG79
* <i>Corynebacterium diphtheriae</i> NCTC 13129					Q6NK15 (DTX)		Q6NIW9						
<i>Mycobacterium smegmatis</i> MC2-155			A0QR55						I7G3G5 I7FXU6				
<i>Streptomyces coelicolor</i> A3(2)		Q9ZBX9	Q9RD91	Q9L0X0	Q9L1E4 (SCO5461)	Q9RD02	Q9ZBG3	Q9X7P1	Q9RI89 Q9S2Y4 Q9S2Y5 Q9S2Y6 Q9S2Y7 Q9S234 Q9KZZ1 Q69985				
<i>Thermomonaspora curvata</i> DSM 43183				D1A8C8		D1AC29	D1A4P7		D1ACW1				
<i>Lysinibacillus sphaericus</i> CBAM5					W7RU68 (MTX)				W7RN56				
<i>Oceanobacillus iheyensis</i> HTE831							Q8EP31						
* <i>Streptococcus pyogenes</i> serotype M5 (str. Manfredo)											P0DN71 P0DN70		
<i>Butyrivibrio proteoclasticus</i> B316	E0S444	E0S332				E0S3P6	E0RWT2	E0S3I2					
* <i>Clostridioides difficile</i> CD160	T3DQ72					T3D766	T3DIR9						
<i>Clostridium thermocellum</i> ATCC 27405		A3DJX6					A3DH36		A3DJ25				
<i>Deinococcus radiodurans</i> R1		Q9RRR1		Q9RXR5		Q9RZM4	Q9RS39						
<i>Thermus aquaticus</i> Y51MC23							B7AC87			B7A853 B7A854			
* <i>Fusobacterium mortiferum</i> ATCC 9817		C3WDX4						C3WDV1					
<i>Herpetosiphon aurantiacus</i> ATCC 23779	A9B244	A9B356		A9B3N6		A9B5M8	A9B0G8 A9B4A3	A9AYL7	A9AYM4 A9B4F2 A9B2Y6				
<i>Thermotoga maritima</i> MSB8					Q9WYW0 (sirtuin)		Q9WYX8						

Bacterial species are representatives of several bacterial phyla: Proteobacteria (red), Actinobacteria (blue), Firmicutes (green), Deinococcus-Thermus (violet), Fusobacteria, Chloroflexi and Thermotogae, respectively. Pathogenic bacteria are marked with a star. Proteins are designated with UniProt accession numbers.

key catalytic residues, it is the H-Y-E in the DTX family and the R-S-E in the CTX family. The characteristic trio became the motif by which other ARTs are designated to the particular family, although their catalytic residues still might differ (Table 1, Figs. 2 and 3).

Bacterial ARTs were originally discovered as toxins, with the ability to irreversibly modify the host's single target protein on a defined residue with high specificity (Table 1). The host targets are usually the key regulators of cellular function and interference in their activity, caused by ADP-ribosylation, leads to serious deregulation of key cellular processes and eventual cell death. The vast majority of bacterial and viral ARTs are enzymes that can MARYlate their targets, but some DTX ARTs have PARYlation activity (PARPs). The specificity of bacterial ARTs is still an ongoing issue, but there is evidence that the CTX family has a structural element - ADP-ribosylating toxin turn-turn (ARTT) loop with eight residues motif X-X-φ-X-X-E/Q-X-E (φ stands for either of aromatic residues (Phe, Trp, or Tyr)) defining the substrate recognition site. DTX family lacks the ARTT loop, so their substrate recognition site is still elusive (the subject is reviewed in [27]).

Of note is that despite the notoriety of many ARTs acting as toxins that participate in pathogenicity, many diphtheria- and cholera-like toxins are being used in a variety of novel therapeutic (e.g. targeted drug delivery) and basic science applications (summarized in [22]).

## 2.1. Diphtheria toxin family ARTs

The founder of the DTX family is responsible for the lethality of *Corynebacterium diphtheria*, the pathogenic bacterium that causes diphtheria. Alternatively, this family is therefore also called ARTD [31]. These ARTs have a comparatively broad target range with acidic (glutamate/aspartate), thiol (cysteine), and hydroxyl (serine/tyrosine)-containing residues among others being described as acceptors [32–37].

The typical DTX family ART fold is augmented by C-terminal extension [2]. The key glutamate is sitting in [QED] sequence. The position of this sequence is suggested to play a role in recognition of the target moiety that is being ADP-ribosylated [38–40].

The DTX family consist of classical toxins, closely related to the original DTX, the family of bacterial PARPs and bacteria-specific antibiotic inactivating ARTs.

### 2.1.1. Diphtheria and diphtheria-like toxins

The classical DTX and closely related toxins are scarcely represented among bacterial genomes [41] ~60 kDa ARTs consisting of three structural domains of equivalent sizes: the catalytic (C) domain forming the fragment A and the translocation or transmembrane (T) domain which with the receptor-binding (R) domain, forming the fragment B [42] (Table 1).

## ARTs

## DTX family

DTX 15MENFSSYHGTPKPGYVDSI--- 47YDDDWKGEYSTDNKYDAAG---144GSSSVVEYINNWEQAKAALS  
 HaPARP 285SNTQLLFHGTAGQNVRIH---316GRMFGHGIYFANKATKSTN---390KLQYDEFIVYQSAQQTIR  
 CdPARP 315GNVVNLFHGSRNANLVGI---351GQMFGNGIYTASKCTKSAL---423YLKNTFIVYNTNQIRIR  
 BpPARP 375KGTKLLFHGSRNENWISI---407GKAFGQGIYFALSADKSFG---486SFVRDEIVFYHESAMTIR  
 MaPARP 289KHSRELWHGTTAGNVLSI---325GRMFGDGVYFSDQSTKSLN---412GVMNNEMIVWRTDQIKIT  
 MsArr 12HESGAYLHGTPKAEKLVGD--- 41AGRIMNHITITQTLDAAVW--- 79GAIEDDPNVTDKKLPGNP  
 SCO2860 5LDEGPFHGHGTPKADLRVGD--- 34PEILMNHITITFALRDGAGL---119WRERLDAMRLEGRAEITIN

## CTX family

CTX 45ANDDKLYRADSRPPDEIK--- 98VRHDDGVVSTISLRSABL---152HPDEQEVSAAGGIPYSQI  
 Scabin 75TTCGTLRYSDSRGPVAVF---114VNQPSPIVSTTYDHDLYKT---160WADQVEVAFPGGIRTEFV  
 LsMTX 90DNEHRLRLWRDRPPNDIF---134TNSPSIFVSTTRARYNNLG---192FPNDEEITFPGGIRPEFI  
 Alt 471PKGITLYRSQRMLPS-IY---495VFYFRNFVSTSLYPNIFGT---571PSNEMEVLPRGLMVKVN  
 ModA 65PNDKPLWRGVPAETKQVL---101KNIALHFAAGLEYNTQVIF---160VSDEQEVMIAPAGSVFRIA  
 SpTre1 349AYNGETIRG-TTLPAHIL---373TVSDGGFMSTSAKTPFDGD---410YKNEAEVLYPPNTRFEVI  
 RrDraT 184ESALLLYRGVNDFTHEQM---211VVRMNNLVSFSSDRGVADC---256LKGEGEYLVIGGDYLVKA  
 LpSdeA 759KPPTRLRERGLNLSEEFK---812KMSGRTNASTTTEIKLVKE---857EGTSEFSVYLPEDVALV

## Divergent ARTs

CtTpt1 94CPPEVLYHGTAARRFVKSI---117QPQGRQYVHLSADVETALQ---163LGNDKVVWLADAIPSKYIR  
 SCO3953 92TPPPYLYHGTVARHLEAI---115RPMNRHDVHLSPDRETATR---160VSANGVWLTQHVPSTRYL  
 PaAcrIF11 1MSMELEHGSYEEISEIR--- 21VFGGLFGAHEKETALSHGE---110SVEMEDEHGTTWLCLPGC  
 SsParT 1MTTSFWRIATDARTYEA--- 33NEVCVAIVYAASSRALACL---125VPEETNLLINPAHPDAKG  
 TaDarT 155EKKQAEFLVKDFFPWEIV

## ARHs

## Macrodomain family

TcPARG 129ACLNFASAEHPGGGFLSGAHAQEE---253RLVLGAWGCGVFGNDPAQVAE  
 DrPARG 89AALNFASAKNPGGGFLGGAQAQEE---217HLVLGAWGCGVFRNDPAGVAR  
 EcYmdB 19VIVNAANPSLMGGGGVDGAIHRAA---115SVAFPAISTGVYGYPRAAAAE  
 OiMacroD 24VIVNAANGSLLGGGGVDGAIHHAA---123SISFPSISTGVYGYPIHEAAA  
 SCO6450 18AIVNAANSSLLGGGGVDGAIHRRG---115TVAFPAISTGVYRWPMDDAAR  
 SC2MacroD 34VVVNAANVYLKHGGGVAGALNKAT---121VLLAPLLSAGIFGADPIHSLR  
 TaDarG 16ALVNTVNTVGVGMKGVALQFKRAF--- 74IFNFPTKKHW---110SIALPPLGAGNGGLPWPEVKQ  
 FmTARG1 17YYAHCISRDIYALGAGIAVEFDKRY--- 67VFNLITKEKY---104KLMPKIGCGGLDRLSWCKVEP  
 SCO6735 21MIAHVCNDLGGWGKGFVLAVSRRW---119SVHLPRIGCGGLAGGTWSRVEP

## DraG-like family

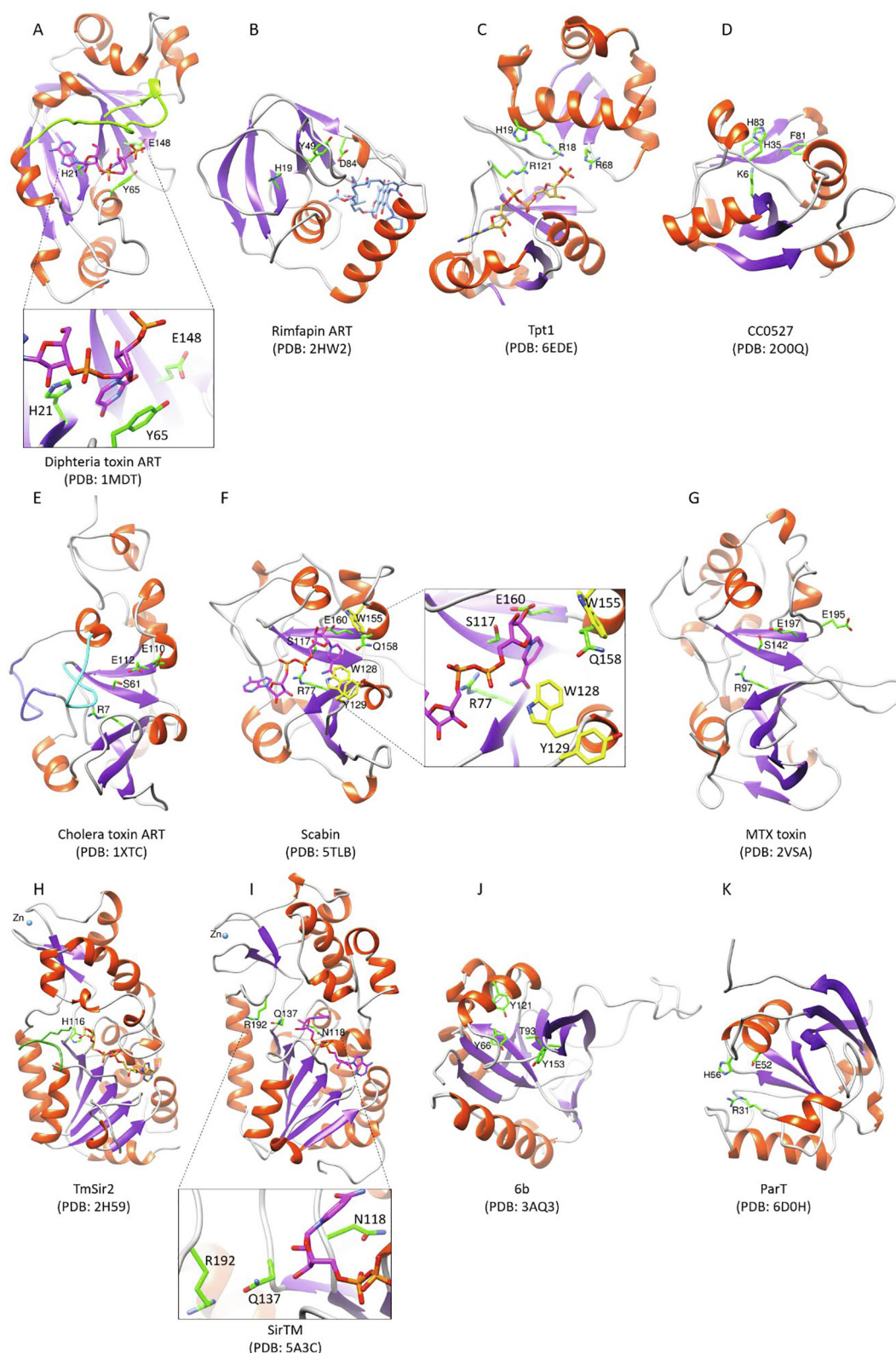
RrDraG 15LGLAVGDALGATVEF--- 45MTGGGWLRKPGQITDDTEMSIAL--- 94RPVDVGNTCRRGIRRYM  
 SpTri1 77VGLAIGDAIGTTIEF---102MVGGGPFRLOPGEWTDTSMAICL---158RCFDIGNTTTRNALEQYL

**Fig. 2. Protein sequence alignments of ART and ARH representatives.** ART alignments include partial sequences of diphtheria (DTX) and cholera (CTX) toxins, PARPs from *Herpetosiphon aurantiacus* (HaPARP), *Clostridioides difficile* CD160 (CdPARP), *Butyrivibrio proteoclasticus* (BpPARP), *Mycobacteroides abscessus* (MaPARP), Arr from *Mycobacterium smegmatis* (MsArr) and its homologue from *Streptomyces coelicolor* (SCO2860), Scabin from *Streptomyces scabiei*, the mosquitocidal toxin from *Lysinibacillus sphaericus* (LsMTX), viral ARTs Alt and ModA from *Escherichia virus T4* and AcrIF11 from *Pseudomonas aeruginosa* PA14 (PaAcrIF11), Tre1 from *Serratia proteamaculans* (SpTre1), DraT from *Rhodospirillum rubrum* (RrDraT), SdeA from *Legionella pneumophila* (LpSdeA), Tpt1 from *Clostridium thermocellum* (CtTpt1) and *S. coelicolor* (SCO3953), ParT from *Sphingobium* sp. (SsParT) and DarT from *Thermus aquaticus* (TaDarT). ARH alignments include partial sequences of PARGs from *Thermomonospora curvata* (TcPARG) and *Deinococcus radiodurans* (DrPARG), MacroD-like proteins from *Escherichia coli* (EcYmdB), *Oceanobacillus iheyensis* (OiMacroD), *S. coelicolor* (SCO6450) and SARS-CoV-2 virus (SC2MacroD), DarG from *T. aquaticus* (TaDarG), TARG1 from *Fusobacterium mortiferum* (FmTARG1) and SCO6735 from *S. coelicolor* and DraG-like proteins from *Rhodospirillum rubrum* (RrDraG) and *Serratia proteamaculans* (SpTri1). Amino acids in motifs characteristic for particular ART/ARH groups are framed.

The DTX, closely related *Pseudomonas aeruginosa* exotoxin A (ExoA) and Cholix toxin from *Vibrio cholerae* [22] all exclusively modify eukaryotic GTP-binding elongation factor 2 (EF2), a protein essential for protein synthesis. The specific target is the intracyclic NH in diphthamide (Fig. 1), a post-translationally modified histidine residue, found in EF2 in archaea, yeast and mammals (diphthamide 715 [43]). The diphthamide is positioned close to the anticodon recognition domain of EF2 and the region interacting with the P-site of the ribosome, so the ADPr probably causes steric hindrances leaving EF2 unable to achieve key interactions and fulfil

its function [22,44]. Consequently, EF2 halts protein production entirely and leads to cell death. The ADP-ribosylation of EF2 is irreversible and cannot be rescued by any endogenous mechanism in the cell [45].

The DTX active site is located in C-domain and positioned in a cleft formed by three  $\beta$ -strands,  $\alpha$ -helix and a flexible loop CL2. In this cleft, His21 and Tyr65 are implicated in  $\text{NAD}^+$  binding and Glu148 plays a key role in catalysis [42] (Fig. 3A). The well-ordered CL2 loop extends over the active site but becomes disordered upon  $\text{NAD}^+$  binding. This allows better positioning of



**Fig. 3. 3D structures of diverse bacterial ARTs.** (A) DTX:NAD complex - CL2 loop (res 34–52) is shown in green; (B) *M. smegmatis* rifampin ART in complex with rifampin (blue); (C) *C. thermocellum* Tpt1 in complex with ADPr analogue (yellow); (D) *C. crescentum* CC0527 (E) CTX - “activation loop” and “active site loop” are shown in dark blue and cyan, respectively; (F) *S. scabiei* Scabin toxin in the complex with NADH - missing Tyr128 was built using UCSF Chimera, amino acids important for DNA binding are shown in yellow; (G) *L. sphaericus* MTX - missing loop was built using Swiss Model; (H) *T. maritima* Sir2 in complex with ADPr (yellow) and an acetylated p53 peptide (olive green), important His116 mutated to alanine was built with UCSF Chimera. (I) *S. pyogenes* SirTM in complex with NAD -  $Zn^{2+}$  ion is depicted as ball model in blue; (J) *A. tumefaciens* 6b apoprotein - missing flexible loop was built with Swiss Model; (K) *Sphingobium* sp. ParT toxin. Key catalytic residues are shown as a stick model in green. NAD<sup>+</sup> and its analogues are shown in magenta. (For interpretation of the references to colour in this figure legend, the reader is referred to the web version of this article.)

NAD<sup>+</sup> and exposes more negative charge that keeps the positively charged diphthamide moiety stabilised and coordinated during the ART reaction [40]. The ADP-ribosylation reaction has been proposed to proceed by a direct displacement reaction, with the  $\pi$ -imidazole nitrogen of diphthamide being activated by Glu148 for nucleophilic attack on the N-glycosidic bond of NAD<sup>+</sup> [42].

A small divergent group of DTX-like ARTs comprising of *Salmonella bongori* SboC/SeoC and *Escherichia coli* EspJ show activity towards Src (Glu310) and Csk (Glu236) host kinases [46–47]. The MARYlation of the two kinases inhibits the phagocytic killing of bacteria by the host cell allowing their persistence in the susceptible host [47]. Of note is that the mART activity of EspJ is linked to its simultaneous amidation activity [46]. The EspJ and SboC/SeoC seem structurally similar to *Pseudomonas syringae* (plant pathogen) AvrPphF effector protein which instead of the key catalytic histidine and glutamate, has Arg72 (Arg79 in SboC/SeoC) and Asp174 (Asp187 in SboC/SeoC) which could participate in the catalytic activity [48–49].

### 2.1.2. Bacterial PARPs

Bacterial PARPs are the only DTX family ARTs that have PARylation activity. Many bacterial species possess proteins essential for a functional PAR metabolism (Table 3) that were probably gained through horizontal gene transfer [4,50]. The human PARP1 and bacterial PARPs from *Herpetosiphon aurantiacus* and *Clostridiodes difficile* seem, indeed, structurally very similar [3,50]. Bacterial PARPs consist of maximum three domains – the N-terminal tryptophan-glycine-arginine (WGR) domain which is important for DNA-dependent activation, the mid-portion with an  $\alpha$ -helix allosteric regulation domain (PARP<sub>reg</sub>), followed by the ART domain (PARP) with the conserved catalytic glutamate (Table 1). The seventy-two sequences containing at least the PARP catalytic domain are found distributed in six bacterial phyla (Actinobacteria, Bacteroidetes, Chloflexi, Cyanobacteria, Firmicutes, and Proteobacteria). Most of these contain the catalytic and WGR domains without a well-defined regulatory domain, although the presence of a helical domain in their 3D predicted structures might fulfil the role [50].

Nevertheless, there is little evidence of actual bacterial PARP activity. Tangible evidence of endogenous PARP activity comes from *Deinococcus radiodurans* where the presence of endogenous PAR was shown [51]. Also, the PAR signal strength was significantly increased when *D. radiodurans* culture was supplemented with NAD<sup>+</sup> or PARG gene was deleted, indicating that the PARylation depends on the NAD<sup>+</sup> availability/metabolism. However, no protein has been identified to be responsible for this activity. PARP activity *in vitro* has been shown for two bacterial PARPs from *Herpetosiphon aurantiacus* and *Clostridiodes difficile* CD160 [4,50]. HaPARP is sensitive to the PARP inhibitor KU-0058948 and required DNA for its activation [4], which is in line with the human PARP characteristics. CdPARP was proven to be highly active *in vitro*. Also, the PARylation by CdPARP and HaPARP was reversed by their corresponding PAR-glycohydrolases as evidence of functional PAR systems in *C. difficile* C160 and *H. aurantiacus* [4,50].

### 2.1.3. Rifampin ARTs

Rifampin ARTs (also called Arr) can be found in the genomes of pathogenic and non-pathogenic bacteria [52]. Arr ADP-ribosylates the hydroxyl group of rifampin (Fig. 1). This modification inactivates rifampin, an antibiotic mainly used for treating tuberculosis and infections caused by multidrug-resistant *Staphylococcus aureus*. Shin et al metagenomics study on the distribution of the Arr gene in search for novel resistant bacterial strains, is a good example of how useful the knowledge on bacterial ARTs can be [52].

Arr is an unusually small enzyme (~16 kDa) and does not have any obvious sequence conservation with known ARTs. Structurally,

it folds similarly to DTX, but the key glutamate residue in the conserved motif H-Y-E is replaced by an aspartate residue (Table 1 and Fig. 2). It is composed of two antiparallel  $\beta$ -sheets and two  $\alpha$ -helices. The two  $\alpha$ -helices form the walls of a deep rifampin-binding cleft (Fig. 3B). The second helix ( $\alpha$ 2) forms a C-terminal loop extension providing a cap over the active site which ensures overall wrapping of the C-terminal region around the core domain and rifampin binding. Given the limited contact that  $\alpha$ 2 makes with the rest of the protein, it is likely that this helix would be unstructured in the absence of rifampin. Interestingly, the crystal structure revealed that rifampin does not make any H-bonds with the active site, its binding is mainly electrostatic. It is suggested that the reaction mechanism proceeds through an oxocarbenium transition state stabilised by Asp84 and formed after releasing nicotinamide. This enables the attack of the hydroxyl group at antibiotic C23 atom to the C1 atom of the distal ribose [38].

The lack of direct interactions of rifampin with Arr, the Arr broad specificity and broad Arr gene distribution in microbial genomes, suggests that the function of Arr against rifampin is only a secondary function [38]. In the study of non-pathogenic environmental mycobacteria, *Mycobacterium smegmatis* Arr is shown to be involved in DNA damage response, reactive oxygen species formation during exponential growth and biofilm formation [53–55]. *Streptomyces coelicolor* also has a rifampin-inactivating Arr homologue, the SCO2860 protein [38].

### 2.2. Cholera toxin family ARTs

The best known bacterial toxin from this group is the infamous CTX from *Vibrio cholerae*, a reason why this group is alternatively called the ARTC group [31]. The active site of the CTX family is characterized by the R-S-E triad which is seen in several bacterial toxins and bacteriophage ARTs (discussed below) (Table 1). The arginine positions NAD<sup>+</sup> in the active site and the [STS] motif (encompassing the serine in R-S-E) stabilizes the NAD<sup>+</sup>-binding pocket. The invariant glutamate positions the NAD<sup>+</sup> molecule to promote hydrolysis, like in the DTX toxins. The CTX family MARYlates arginine, lysine, cysteine, aspartate and asparagine [56–60] (examples mentioned below). A small group of guanine-specific ADP-ribosylating toxins found in cabbage butterfly and some insecticidal and soil-dwelling bacteria target DNA instead [61–65].

#### 2.2.1. Cholera and cholera-like toxins

CTX and closely related toxins are, as DTX toxins, scarcely represented in bacterial genomes and come in three types of structural-functional organisations.

The first group, the typical cholera toxins, include CTX, the heat-labile enterotoxin from *Escherichia coli* [66] and the pertussis toxin from *Bordetella pertussis* [67–68]. They are two-chain proteins (Mr = 85,6 kDa), with an enzyme component A, and a nontoxic host receptor-binding component B. The group is structurally distinguished by a long loop which helps to anchor the catalytic subunit into the B pentamer during toxin delivery.

Activation of the enzymatic A subunit requires proteolytic cleavage between residues 192 and 194, reduction of a single disulphide bond (Cys187 - Cys199) which holds the nicked A subunit together, and a subsequent gain in flexibility of an “active site loop” which occludes active site by interacting with an “activation loop” [69–71] (Fig. 3E). “Active site loop” increased flexibility leads to an open conformation and permits entry of the NAD<sup>+</sup> and the target arginine residue [72]. The substrate of these toxins is the  $\alpha$  subunit of the heterotrimeric G-protein (CTX modifies Arg201, pertussis toxin modifies Cys347 and *E. coli* toxin targets Lys345 and Asn347) [56,73]. MARYlation locks the G protein in a GTP-bound state, which constitutively stimulates host adenylate cyclase and causes efflux of the chloride ions together with water causing the

typical diarrhoea [22,67]. Active-site residues Arg7, Ser61 and Glu110 are implicated in substrate binding and Glu112 is a catalytic residue that likely participates in the formation of an oxocarbenium-like intermediate of  $\text{NAD}^+$  that is capable of reacting with an incoming nucleophile [74]. Two mutually similar toxins from *Salmonella* serovar Typhi (typhoid toxin) [75] and Typhimurium (ArtAB toxin) [49,76–77] share structural similarity to pertussis toxin, but show some dissimilarity in the structural organization (typhoid toxin incorporates domains with nuclease and ART activity) and symptoms (ArtAB, unlike pertussis toxin, does not induce leukocytosis [76]), and would therefore be an interesting subject for future studies.

The second type of CTX-like toxins from pathogenic *Clostridium botulinum*, *Clostridium perfringens* (iota toxin) [78] and facultative pathogen *Bacillus cereus* (certhrax) [79] have a catalytic domain and receptor binding domain which are expressed separately and interact on the surface of the host cells. They target monomeric G-actin at Arg177 which inhibits actin polymerization, causes cytoskeleton breakdown and cell death [22]. These ARTs often come in operons with immunity proteins which suggests a role in both intra-bacterial and bacterio-eukaryotic conflicts [80].

The third and smallest type of CTX-like toxins includes *Staphylococcus aureus* C3stau2 [81], *C. botulinum* C3bot [82] and *Pseudomonas aeruginosa* ExoS [83] which consist only of the catalytic domain. C3 toxin-mediated MARYlation occurs on Asn41 of small Rho GTPases, which also play a role in cytoskeleton dynamics and gene expression. This MARYlation does not inhibit the Rho proteins but sequesters them to the cytoplasm and therefore makes some of the usual interactions inaccessible [22].

### 2.2.2. Pierisins

Pierisin and the pierisin-like ARTs are a small group of CTX family toxins that mainly target DNA. The founder, pierisin, is found in the cabbage butterfly species, *Pieris rapae*, where it seems to act antagonistically towards the non-habitual parasitoids [61,64]. Pierisin MARYlates the N2 atom of guanine bases of dsDNA, causing apoptosis of the target cell [61,84–85].

Scabin from *Streptomyces scabies* (a soil-dwelling plant pathogen) is a 22 kDa single-domain enzyme that shares 40% sequence identity with pierisin, but it lacks the pierisin-characteristic Ricin B-like domain and the auto-inhibitory linker (Table 1, and exemplified by MTX explained below and in Fig. 3G), suggesting a different regulatory mechanism [86]. Scabin was shown to MARYlate the exocyclic amino group on guanine bases and most of its derivatives in either single-stranded or double-stranded DNA [86–87]. The Trp128 and Tyr129 bind DNA substrate by interacting with adjacent nucleotides to the guanine nucleophile, allowing Trp155 to dock the target guanine base making it required for transferase activity (Fig. 3F) [87,199]. Glu160 stabilizes the oxocarbenium ion intermediate, while Gln158 positions guanine N2 exocyclic amine for nucleophilic attack on C1' atom of  $\text{NAD}^+$  distal ribose [87–88].

*S. coelicolor* pierisin-like ART SCO5461 (ScARP) shares a high structural similarity with Scabin (RMSD = 0.484 Å) and has 78.4% sequence identity. Amino acids important for Scabin catalysis are also present in SCO5461, therefore, the same catalytic mechanism is proposed [89]. It is predicted to be a transmembrane protein with a transmembrane domain (T) and an extracellular catalytic domain (Enterotoxin\_a; Table 1). SCO5461 MARYlates primarily guanosine and most of its derivatives, as well as yeast tRNA [63], and can be auto-modified on Asp161 [21]. Depletion mutant showed pleiotropic conditional defects in morphological differentiation, sporulation, and highly increased production of antibiotic actinorhodin [15].

Protein-modifying pierisin homologue with 31% sequence identity to pierisin is the mosquitocidal toxin from *Lysinibacillus sphaericus* (an insect pathogen), also called MTX. It is structurally rather

well studied ~97 kDa single-chain toxin with an N-terminal catalytic ART domain (Enterotoxin\_a) and C-terminal putative Ricin B-like domains typical for pierisin and similar ARTs (Table 1, Fig. 3G) [200]. The linker between the two domains has an inhibitory function, and the MTX can be activated by proteolytic cleavage which, *in vivo*, occurs in the host mosquito larval gut [65]. Heterologous expression of MTX in *E. coli* yielded several MARYlated proteins, out of which one was the translation elongation factor EF-Tu (on undetermined arginine residue). The MARYlation of EF-Tu prevents the ternary complex formation of EF-Tu, GTP, and aminoacyl-tRNA, resulting in inhibition of bacterial protein synthesis [90]. MTX shares a characteristic [EXE] catalytic motif (Fig. 3G) common in other arginine-modifying ARTs [60,88].

### 2.2.3. Viral ARTs

The three known viral ARTs produced by the T4 bacteriophage – Alt, ModA and ModB, belong to the CTX family (Table 1 and Fig. 2). The well-ordered production of T4 is achieved by sequential activation of three different classes of promoters and at the post-transcriptional level. The latter relies on the coordinated ADP-ribosylation activity of the three T4 ARTs. The Alt acts immediately after infection and modifies at least 27 *E. coli* proteins [91], including one of the  $\alpha$ -subunits of the RNA polymerase, EF-Tu (mentioned in MTX section above) and MazF at Arg84 (a part of the *E. coli* toxin/antitoxin (TA) system) inhibiting its endonuclease activity. MazE/MazF TA is suggested to be a part of the *E. coli* antiphage defence system as the growth of T4 phage was significantly increased by the disruption of *mazE-mazF* genes [92]. ModA modifies both  $\alpha$ -subunits of the host RNA polymerase at Arg265, reducing its activity [93]. ModB targets ribosomal S1 protein, EF-Tu and six other proteins [91]. Joined MARYlation of translation apparatus (EF-Tu, S1 and others) by Alt and ModB likely contribute to the immediate shut-down of host mRNA translation during T4 infection [91–94].

A novel type of bacteriophage AcrIF11 mART was recently identified as a part of the anti-CRISPRs (Acrs) system, which acts as a protein-based inhibitor able to inactivate the bacterial CRISPR-Cas immune system. Crystal structure of AcrIF11 revealed the best fit with the catalytic domain of DTX, but instead of the H-Y-E motif, only the His residue was conserved (His7), while the tyrosines and catalytic glutamate are replaced by Phe26, His37, and Asp115, respectively (Fig. 2). This newly discovered ART domain has not been annotated yet (Table 1). It is shown that D115A mutation leads to a complete loss of ADP-ribosylation, but does not completely inhibit  $\text{NAD}^+$  binding, suggesting that D115 is essential during the catalytic process. This is in agreement with the same spatial positioning of D115 as core catalytic Glu residues in known bacterial ARTs (Fig. 3). Inhibitory action of AcrIF11 is achieved through MARYlation of the Asn250 residue of the Cas8f subunit of the Csy complex. This completely abolishes its dsDNA binding activity and consequently inactivates the CRISPR system. Interestingly, for substrate recognition, the whole complex composed of nine Cas proteins (Cas5f, Cas6f, Cas8f, and six Cas7f proteins) and a single 60-nt crRNA (CRISPR RNA) is required. Specific double mutation within the Cas7f subunit (K58A/K60A) render the Csy complex resistant to ADP-ribosylation by AcrIF11, while single mutations markedly diminish this modification [95]. This system exists in lysogenic *Pseudomonas aeruginosa* PA14 and in more than 50 other Proteobacteria species.

## 2.3. Divergent ARTs

### 2.3.1. Tpt1/KptA and CC0527 ARTs

Tpt1 (tRNA 2'-phosphotransferase) (also known as KptA in *E. coli*) is one of the most represented lineages in the ART superfamily (Table 3)(reviewed in [96]). Due to its distribution and sim-

ple structure, it is considered the closest to the original ART that likely evolved in bacteria and was then transferred to archaea and eukaryotes, independently [2]. In yeast, it is essential for the maturation of tRNA, by adding the ADPr to the 2'-phosphate, which is exposed after the tRNA splicing and RNA ligase action, following the intron removal [97]. Since bacteria lack introns, its function here is much less obvious. In some bacterial operons, it comes with the RNA repair 5' → 3' polymerase Thg1, which suggests a role in RNA repair. In several bacteria, it comes as a part of NAD<sup>+</sup>/ADPr metabolism operons (with, for example, sirtuins, macrodomains, ARHs, NADAR (NAD<sup>+</sup> and ADPr domain) etc.), but none of the RNA-related genes [73] which indicates substrates other than RNA. *In vitro*, bacterial Tpt1/KptA (from *E. coli* and *S. coelicolor* SCO3953) robustly modifies 5'-phosphorylated RNA, but not the 3'-phosphorylated RNA [98]. The same activity is observed in archaeal and fungal homologues [99]. It is, at this point, not clear how this might be physiologically relevant but suggests that the bacterial system is more versatile and plastic than we might have assumed. Because Tpt1 is inessential in exemplary bacterial and mammalian taxa, Tpt1 is seen as an attractive antifungal target (essential in Fungi and Ascomycota) [100–101].

The overall structure and catalytic activity of Tpt1-like proteins can be best described on Tpt1 protein from *Clostridium thermocellum*. It consists of two globular domains, an N-terminal and a C-terminal domain connected by a long loop (represented together as a PTS<sub>2</sub>-RNA domain in Table 1). N-domain has the winged helix motif (helix-turn-helix family), which is shared by many DNA-binding and some RNA-binding proteins [102]. C-domain consists of two antiparallel β-sheets surrounded by five α-helices, which superimposes well on NAD<sup>+</sup>-binding fold of bacterial (DTX-like) toxins. The characteristic motif of Tpt1/KptA is H-H-h (with h being a hydrophobic residue (Fig. 2)), while the catalytic activity is carried out by four residues – RH-R-R conserved in all Tpt1-like proteins (Fig. 3C). The reaction mechanism is carried out in two steps: first, 2'-phosphate of tRNA performs a nucleophilic attack on C1' of distal ribose in NAD<sup>+</sup> forming a 2'-phospho-ADP-ribosylated RNA intermediate and expelling nicotinamide; second, transesterification of the distal ADPr 2'-OH to the tRNA 2'-phosphate displaces the tRNA product and generates ADPr 1',2'-cyclic phosphate [100,103–105].

CC0527 protein from *Caulobacter crescentus* has a DUF952 domain (Table 1) and shares a similar structure with the Tpt1 C-terminal domain (RMSD between 31 pruned atom pairs is 0.911 Å) although has a very low sequence identity (11.3%). Its active site architecture is characterized by the H-H-h motif. The conserved H and alcoholic residue usually found within an HX[S/T] motif often make polar contacts with the 2'- and 3'-OH of proximal ribose. The hydrophobic residue (h) is found in the proximity of the distal ribose. CC0527 gene is sporadically distributed in bacteria (around 1% of the 200 000 sequenced genomes (RefSeq) and in [2]). Although the structure of *C. crescentus* CC0527 is available (Fig. 3D), its function remains obscure. Aravind and colleagues suggested by the rule of “guilt by association” (where CC0527 sits in operons with genes related to antibiotic ADP-ribosylation) that CC0527 ADP-ribosylates antibiotics or other toxic compounds, probably in a reaction similar to the rifampin ARTs [2,106].

### 2.3.2. 6b/RolB ART

The 6b protein from *Rhizobium radiobacter* (formerly *Agrobacterium rhizogenes*, plant pathogen) is distantly related to the RolB family proteins. The RolB gene has an elusive function in *R. rhizogenes* hairy root disease in plants [107]. The 6b structure adopts an ART toxin fold closely related to CTX and ExoA. The ART activity is seen *in vitro*, but only in the presence of the host *Arabidopsis* protein ARF, and GTP. The 6b represents a new toxin family, with Y-T-Y-Y (Tyr66, Thr93, Tyr121 and Tyr153) as the

ADP-ribosylation catalytic residues [2,108] (Table 1, Fig. 3J). The 6b protein interacts with many different host proteins implicated in plant cell proliferation. Transgenic *Arabidopsis* plants expressing the 6b gene display morphological defects, and more closely, a microRNA (miRNA) deficiency phenotype, meaning 6b could target miRNA processing and splicing machinery [108].

## 3. Sirtuins

Sirtuins are enzymes found in all kingdoms of life. The first sirtuin found was the yeast Sir2, identified as a silencing factor (silencing information regulator) with mild ADP-ribosylation activity [109]. The best-studied sirtuins are the seven mammalian homologues (SIRT 1–7) that seem to act primarily as NAD<sup>+</sup>-dependent deacetylases involved in fundamental processes such as metabolic homeostasis and genome integrity [110]. Later they were found to also remove a wide variety of acyl moieties including butyryl, glutaryl, propionyl-lysine, succinyl and others [111]. Some of them (human SIRT4, 6 and 7) were shown to have additional ART activity by attaching the ADPr moiety to the ε-amine of lysine [109,112] (Fig. 1).

The Sir2 homologues are widespread in bacteria (around 2% of 200 000 genomes sequenced (RefSeq)). *E. coli* and *Salmonella typhimurium* LT2 Sir2 homologues, CobB, were identified as enzymes involved in cobalamin synthesis via its weak ART activity towards a small molecule 5,6-dimethylbenzimidazole, in addition to its robust protein deacetylase activity [113–114].

Better studied in the context of ADP-ribosylation is the *Mycobacterium smegmatis* SIRT4 (MsSIRT4) which exhibits a robust auto ADP-ribosylation activity on arginine (probably Arg33). Studies on the MsSIRT4 deletion mutant showed growth retardation on minimal medium, and the gene transcription was dramatically induced in the wild type strain in the same conditions, suggesting an important role of MsSIRT4 in fundamental metabolism and growth [115].

Structurally, sirtuins are comprised of a highly conserved Rossmann fold (six parallel β-strands forming an extended β-sheet, found in NAD<sup>+</sup>-binding enzymes) and a more diverse zinc coordinating domain (Fig. 3H). Substrate specificity of sirtuins relies on what seems much more than a sequence consensus of the target [111]. The crystal structure of the *Thermotoga maritima* Sir2 (TmSir2) 17.8 kDa monomeric auto-MARylated protein (modified on Asp56) [116] was resolved and gave an insight into the catalytic mechanism. The reaction requires the right orientation of NAD<sup>+</sup> and acetyl-lysine substrate which needs to be in a position to carry out the nucleophilic attack on the C1' atom of distal ribose forming the O-alkylamidate intermediate and releasing nicotinamide. His116 acting as an acid and a base, respectively, ensures the formation of two more subsequent intermediates. In the end, water-mediated attack on last intermediate results with released lysine substrate side chain and 2'-O-acetyl ADPr (OAAADPr). The mechanism is explained in detail in [117].

A very distinct and diverged class of sirtuins that can be found in pathogenic bacteria (e.g. *Staphylococcus aureus* and *Streptococcus pyogenes*) are structurally similar to Sir2 (RMSD = 2.066 Å) (Fig. 3I) but they share only 10.6% sequence identity. These sirtuins (SirTM) come in operons with a specific subclass of macrodomain proteins, which reverse the sirtuin catalysed ADP-ribosylation. SirTM-mediated ADP-ribosylation is dependent on another posttranslational modification – lipoylation. The two PTMs play a role in microbial pathogens response to oxidative stress, which is often used by their hosts as a potent defence mechanism [112]. SirTMs will be discussed further in the context of the reversible ADP-ribosylation systems.

#### 4. ADP-ribosyl hydrolases

Two types of evolutionarily very distinct enzymes can reverse the ADP-ribosylation modification – the macrodomain hydrolases and the hydrolases related to ADP-ribosyl-(dinitrogen reductase) glycohydrolase (DraG) [26]. Also, there are non-canonical ADPr hydrolases [118–119]. The canonical  $\alpha/\beta$  macrodomain fold consists of six-stranded mixed  $\beta$ -sheet sandwiched by five  $\alpha$ -helices. Within the context of de-ADP-ribosylation, the macrodomain group consist of the PAR-glycohydrolase (PARG), MacroD-like and terminal ADPr glycohydrolase 1 (TARG1)-like hydrolases [120]. Canonical PARG cleaves the PAR-specific O-glycosidic ribose–ribose bonds [4], but cannot hydrolyse the last protein-bound ADPr, thus leaving a MARYlated protein (Fig. 1). DraG-like enzymes in eukaryotes (called ARHs) cleave MARYlated proteins on arginine and serine residues, the O-glycosidic bond of PAR chains and OAADPr [121–123]. In eukaryotes both DraG-like and PARGs are recruited to DNA damage sites and are reported to play important parts in the DNA damage response [124–126]. MacroD- and TARG1-like break the O-glycosidic ester bond of modified aspartates, glutamates, and OAADPr, the reaction product of the NAD<sup>+</sup>-dependent sirtuin deacetylases, as well as phosphate ester at nucleic acid ends, thus cleaving off the final ADPr as well [98,120].

##### 4.1. Macrodomain family ARHs

###### 4.1.1. Bacterial MacroD-like ARHs

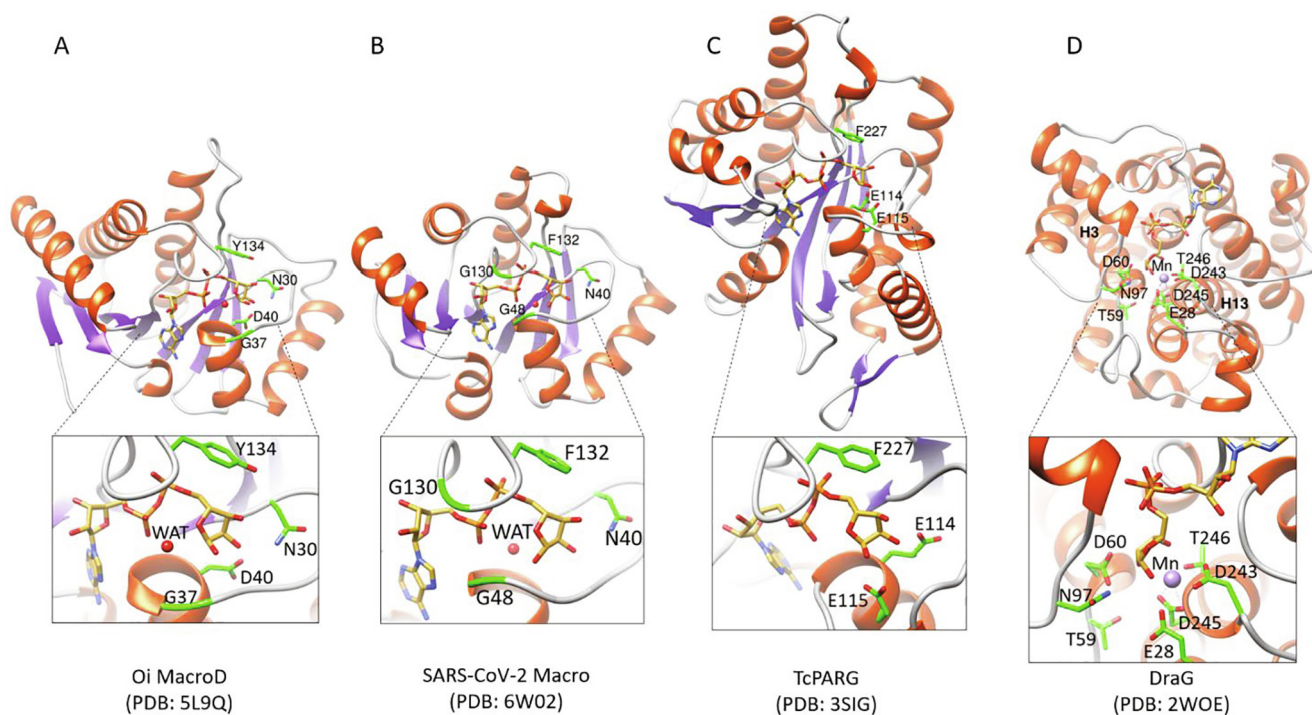
MacroD homologues can be found in most bacteria [120] (Table 3). The typical homologues contain the signature motifs Nx(6)GG[V/L/I]D and G[V/I/A][Y/F]G (Fig. 2), and the catalytic duo Asn174 and Asp184 (in human MACROD1) [127].

MacroD protein from *Oceanobacillus iheyensis* (deep-sea bacterium) is composed of a central seven-stranded mixed  $\beta$ -sheet

sandwiched between the five  $\alpha$ -helices which is very similar to that found in other macrodomains [128] (Fig. 4A). The first proposed catalytic mechanism requires three conserved residues: asparagine that coordinates the nucleophilic water, tyrosine that stabilizes the orientation of the distal ribose and aspartate which deprotonates catalytic water molecule to attack carbonyl group with concomitant hydrolysis of the acetyl group [128–131]. Interestingly, the mutation of this aspartate residue does not manage to completely abolish the enzyme activity, and not all MacroD-like macrodomains possess such aspartate residue. This leads to a proposal of a second, equally possible, substrate assisted mechanism, in which water molecule tightly coordinated between P $\alpha$  and distal ribose is activated by the P $\alpha$  group for nucleophilic attack on the carbonyl carbon [128,132]. Mutation of glycine that positions this water molecule led to a significant fall in catalytic efficiency and proved that it is indispensable for the adequate conformation of ADPr. This latter mechanism seems also to be one of the proposed mechanisms for the catalytic mechanism of the viral macrodomains from Coronaviridae which will be discussed in the next chapter [133–134].

*E. coli* MacroD homologue, YmdB, appears to be a multifunctional protein that regulates a variety of cellular processes; deacetylates OAADPr, hydrolyses MARYlated protein substrates, regulates RNase III activity and modulates bacterial biofilm formation [129,135–137]. The crystal structure of *E. coli* YmdB revealed the catalytic duo made out of Asn25 and Asp35 and an active water molecule which is proposed as the nucleophile to attack the acetyl group of OAADPr [130].

The SCO6450 is an *S. coelicolor* MacroD orthologue. Besides its activity on MARYlated protein substrate, SCO6450 was found to be active at reversing RNA MARYlation mediated by both SCO3953 (*S. coelicolor* homologue of the Tpt1) and the human homologue TRPT1, as well as from MARYlated phosphorylated double-stranded DNA ends [98,138].



**Fig. 4.** 3D structures of bacterial and viral ARHs. (A) *O. iheyensis* macrodomain in complex with ADPr; (B) SARS-CoV-2 macrodomain in complex with ADPr; (C) *T. curvata* PARG in complex with ADPr; (D) *R. rubrum* DraG in complex with ADPr – amino acids that are important for binding of dinuclear Mn<sup>2+</sup> centre are shown (second Mn<sup>2+</sup> ion is not present in the crystal structure). ADPr is depicted as a stick model in yellow, and amino acids that are presumed to be important for catalysis are shown in green. In (A) and (B) catalytically important water molecule is depicted as a ball model. (For interpretation of the references to colour in this figure legend, the reader is referred to the web version of this article.)

#### 4.1.2. Viral MacroD-like ARHs

RNA viruses from families of Coronaviridae [139], Togaviridae [140] and Hepeviridae [141] have macrodomain encoding genes [134,142–144]. They come as a single domain or as a part of big multidomain proteins [7,134]. Most of these viral macrodomains are MacroD homologous [120], except the SARS coronavirus (SARS-CoV) unique SUD macrodomains [120,145].

The viral macrodomains are linked to promoting viral replication and seem to play an important role in deflecting the host's first line of the immune response. Examples come from experiments in bone-marrow-derived macrophage and murine models of murine hepatitis and coronavirus infection. When infected with catalytic-null or macrodomain (from murine hepatitis virus (MHV), human coronavirus 229E (HCoV-229E) and SARS-CoV deletion mutant strain, the viral replication and overall organ viral load were lowered and generally produced milder symptoms [146–148]. As a reaction to corona viral infection, the activity of human antiviral PARPs (PARP9, 12 and 14) goes up and induces the pro-inflammatory response in the cell. Viral macrodomains can reverse this antiviral environment as seen *in vitro* for several viral macrodomains from coronaviruses, alphaviruses and hepatoviruses using the standard model MAR/PARYlated substrates [7,133,146,149]. Another piece of evidence emphasizing the importance of macrodomain-antiviral PARPs interactions comes from the evolutionary study of macrodomains in mosquito alphaviruses. The mosquitos lack the antiviral PARPs in their genomes and sequence comparison of members of the mosquito-specific alphaviruses with closely related alphaviruses of the western equine encephalitis complex revealed a specific loss of catalytically important residues within their macrodomain [134].

The SARS-CoV-2 virus, responsible for the COVID-19 infection belongs to the family of betacoronaviruses and its macrodomain is a part of the non-structural protein 3 (nsp3), a 200 kDa multidomain protein [134,150] (Table 2). Many groups studied the crystal structure and structural phylogenetic approach to define and demonstrate its unique characteristics to enable the search for the inhibitor of the SARS-CoV-2 macrodomain. It has been found that the SARS-CoV-2 macrodomain presents several unique features among which a distinct electrostatic microenvironment, as well as specific residue functionalities and differences in the proximal ribose binding area and catalytic pocket. Also, concerns have been raised about the potential inhibitor targeting human or human microbiome macrodomains. The sequence comparison of the SARS-CoV-2 macrodomain with the human and human microbiome macrodomains showed the best fit with human PARP9 and PARP14, and the Coronaviridae-like macrodomain from the human microbiome *Clostridium tyrobutyricum* YmdB. None of these sequences, however, showed similarities in the proximal ribose binding area, identified as the macrodomain selective region. This shows that alphavirus and SARS-like coronavirus macrodomains can be selectively targeted without a high likelihood of cross-reactivity with the human host or microbiome which lends further argument as to why the viral macrodomains are valuable therapeutic targets [134,142,146,151–153].

The therapeutic potential of the SARS-CoV-2 macrodomain started a rapid search for a potential inhibitor and led to a vast number of crystal structures deposited in Protein Data Bank. Apo form (PDB: 6WEY, 6VXS, 6WEN); complex with ADPr (PDB: 6W02, 6Z5T, 6WOJ, 6YWL), AMP (PDB: 6W6Y), inhibitors of the related PARG enzyme ADP-HPD and ADP-HPM (PDB: 6Z6I and 6Z72, respectively), MES (PDB: 6WCF, 6YWM) and HEPES (PDB: 6YWK). Also, an extensive fragment analysis resulted in 214 crystal structures of SARS-CoV-2 macrodomain in complex with various fragments [153]. This analysis gave extensive information about different fragment binding that could lead to the design of potential specific inhibitors.

While the catalytic mechanism of MacroD-like enzymes is not fully understood, current evidence suggests a substrate-assisted mechanism in which precise positioning of the distal ribose plays an important role [129,132,134]. Crystal structures of SARS-CoV-2 macrodomain in complex with ADPr revealed the presence of a substrate-coordinated, activated water molecule placed between the Gly48 and P $\alpha$ , which was first discovered in a bacterial MacroD-like enzyme [128]. This idea was tested by the introduction of a small side chain at Gly48 (G48V) which led to a reduction in catalytic activity, supporting the idea that a substrate-activated water molecule partakes in the reaction [26]. Amino acids proposed to be involved in catalysis are shown in Fig. 4B.

#### 4.1.3. Bacterial TARG1-like ARHs

TARG1 sequences are scarce (1% of total macrodomain sequences) and only around thirty are found in sequenced bacterial genomes, mostly in Firmicutes (84.8%) and Fusobacteria (6.1%) phyla [154] (Table 3). It is a small, 17 kDa macrodomain protein that occupies a distinct branch in the phylogenetic tree [120]. Despite its low sequence homology to MacroD-like proteins TARG1 exhibits a canonical core fold similar to other macrodomain proteins but lacks the extended N- and C-terminal structural elements found in MacroD. TARG1 catalytic duo encompasses Lys84 and Asp125 in human TARG1 [155–156].

Using bioinformatics and phylogenetic analysis, *Fusobacterium mortiferum* (usually pathogenic) TARG1 (FmTARG1) was recently described. It is the first bacterial macrodomain protein shown to be capable of deacetylating, de-MARYlating and de-PARYlating. Its efficiency for OAADPr is even higher than human TARG1 and other bacterial macrodomains (OimacroD, YmdB and *Staphylococcus aureus* SAV0325). The FmTARG1 gene is located in a unique operonic context, (found in *Fusobacterium perfoetens* as well), which includes an immunity protein 51 domain, typical of bacterial polymorphic toxin systems, making it a likely TA system [154].

*S. coelicolor* enzyme SCO6735 is a macrodomain protein that groups into TARG1/ALC1 branch but lacks the catalytic duo, therefore the catalytic mechanism is probably unique for the SCO6735 macrodomain subclass. Nevertheless, in the *in vitro* assays, SCO6735 can remove MARYlation from glutamate residues. It seems to be involved in DNA damage response as its expression is under the control of RecA-independent DNA damage-inducible promoter and upregulated upon UV-induced DNA damage [21,157–158]. Also, disruption of SCO6735 increases the production of actinorhodin antibiotic which indicates its possible regulatory role in antibiotic metabolism [21]. Our ongoing study tackles the catalytic mechanism of SCO6735 by molecular dynamics simulations of the protein in complex with ADPr and cognate substrate.

A specific macrodomain hydrolase that also belongs to this group is the antitoxin DarG from TA system DarT/DarG, described in more detail in the reversible ADP-ribosylation systems below.

#### 4.1.4. Bacterial PARGs

Bacteria were historically considered to be devoid of PAR metabolism, despite the fact many harbour genes homologous to the eukaryotic PARPs and PARGs [3]. Many bacteria possess a distant PARG homologue denoted as DUF2263 (Table 2 and 3). The first solved crystal structure of such a protein was the one from *Thermomonospora curvata* (Fig. 4C). Comparison with the available structures revealed an ADPr-binding macrodomain fold with a novel type of N-terminal helical extension [4]. Its catalytic domain belongs as a distant member of the macrodomain protein family. It contains the PARG signature sequence (GGG-X<sub>6-8</sub>-QEE) with previously identified key residues: two consecutive glutamates (Fig. 2) [4,159–160]. One of those signature glutamates mediates nucleophilic attack of the putative oxocarbenium intermediate by a

nearby water molecule, which results in the release of free ADPr. Indeed, several PARGs from different bacterial species (including *T. curvata* (TcPARG) and *H. aurantiacus* (HaPARG)) can hydrolyse PAR as seen *in vitro* [4].

TcPARG can bind only to the terminal residue of PAR polymers because of the so-called ribose cap near its C-terminus. Therefore, the bacterial-type PARGs are believed to be confined only to act as *exo*-glycohydrolases. The eukaryotic, or canonical, PARGs share a highly similar mechanism of hydrolysis of PAR with bacterial-type PARGs but can process PAR in both *endo*- and *exo*-mode due to the lack of such steric hindrance, i.e., the ribose cap [161]. Albeit, the canonical PARGs have phenylalanine (Phe398 in *Tetrahymena thermophila*; Phe902 in human PARG) [162] which positions next to distal ribose and lowers the affinity to PAR in *endo*-mode, restricting them to predominantly act as *exo*-glycohydrolases [34].

Recently, the *Deinococcus radiodurans* PARG (DrPARG), similar to HaPARG and TcPARG, was also characterised [51]. The authors observed that an extra  $n + 1$  ADPr unit could fit in the protein surface, likely due to the lack of mentioned steric hindrance. This was corroborated by *in vitro* assays, proving that, in addition to the *exo*-, the DrPARG also has an *endo*-glycohydrolase activity. Expression of DrPARG is upregulated after radiation damage and endogenous PAR was accumulated after UV damage. Recovery after was somewhat compromised in the DrPARG depletion strain [51]. Both, the *endo*- and *exo*-activity and involvement in DNA damage response make DrPARG very similar to human PARG [163].

PARG and MacroD homologue form a basic hydrolase duo that accompanies PARPs from *H. aurantiacus*, *C. difficile* and *Butyrivibrio proteoclasticus* (Table 3) ensuring complete de-PARylation. Moreover, *B. proteoclasticus* and *H. aurantiacus* possess one and even more additional hydrolases, respectively. This diverse set of proteins for complete functional PAR metabolism present in these bacteria are more likely an adaptive advantage that has been preserved over time, rather than a simple horizontal gene transfer event [50]. For *H. aurantiacus* it might reflect its specific way of life as nature's scavenger and a predator of other bacteria [164–165].

#### 4.2. DraG-like family ARHs

DraG family of hydrolases is named after its founder DraG protein found in nitrogen-fixing bacteria. Its homologues are present in all kingdoms of life. In bacteria, it is best studied in *Azospirillum brasilense* and *Rhodospirillum rubrum*, where it regulates the nitrogen fixation metabolism. There are three DraG homologues encoded in the human genome, ARH1–3 [26,121,166–167]. The specificity of the well characterised DraG-like hydrolases is to cleave the linkages to arginine and serine [168–169]. DraG acts specifically towards MARYlated substrates and is most probably active as a monomer. Structures of the DraG from *A. brasilense* and *R. rubrum* have been solved, and they have high structure similarity (RMSD = 0.845 Å and 60% of sequence identity) [166,170–171]. The crystal structure shows 15 all- $\alpha$ -helix architecture with two magnesium ions located in the active site (although the protein shows the best activity when  $Mn^{2+}$  is bound) (Fig. 4D). Comparison of the *A. brasilense* DraG with other similar ARHs (2FOZ,1T5J and 2CWC) shows that 13 of those helices define a common  $\alpha$ -helical core structure of the DraG family. Central helices H3 and H13 carry the highly conserved asparagine and threonine residues that are critical for  $Mn^{2+}$  binding. The binding model shows that the manganese ions have a crucial role in positioning and activating the terminal ribose unit for nucleophilic attack by a water molecule [166].

Based on experiments and crystal structure of DraG from *R. rubrum* in complex with ADPr it was proposed that catalytic reaction is initiated by opening of the ribose ring and formation of a protonated Schiff base. This substrate opening leads to the shift

in metal coordination, thus allowing the nucleophilic attack by a water molecule activated by  $Mn^{2+}$  and resulting in a tetrahedral intermediate. Finally, the proton transfer via Asp97 results in a better leaving group, promoting intermediate collapse, releasing of arginine and ring closure of an open ribose [171].

Since DraG comes in a pair with its cognate ART, the DraT, they will be mentioned further in the reversible ADP-ribosylation system context.

### 5. Reversible ADP-ribosylation systems

Bacterial reversible ADP-ribosylation systems, in general, encompass transferase/hydrolase pairs that work together, i.e., counteract each other, and lie in the same operon. They usually represent a TA pair, where the toxin is aimed at the host/enemy and the antitoxin is the antidote that protects the assailant, the bacteria. TA systems are also considered important as a bacterial persistence mechanism. Under stress conditions, the antitoxin is inactivated leading to cell growth arrest due to toxin activation. In favourable growth conditions, the antitoxin gets activated and cell proliferation resumes. There are exceptions to these classical TA systems, as exemplified by some of the systems explained below.

#### 5.1. DraT/DraG

DraT/DraG is one of the earliest discovered ART/ARH pairs. While DraT homologues are restricted to several nitrogen-fixing bacteria, DraG homologues can be found in all three domains of life [172].

The biological nitrogen fixation by conversion into ammonia is highly energetically costly, therefore the system is tightly regulated both on the transcriptional and post-translational level. The DraT (dinitrogenase reductase ADPr transferase) MARYlates the Arg101 residue of the key enzyme in nitrogen fixation Fe protein (dinitrogenase reductase) during the “switch-off” phase [173] which prevents the formation of the nitrogenase complex and consequently reduces nitrogen fixation. The “switch-off” state is induced by high levels of ammonia or during low energy conditions (due to light or oxygen deprivation) [174]. DraT activity is counteracted by its neighbouring hydrolase DraG (see above) residing in the same operon. The pair is simultaneously expressed at low levels, but their activity is tightly regulated. DraG is inactivated by sequestration to the bacterial plasma membrane and becomes activated during the normal nitrogen fixation conditions (while DraT is inactive) [80,175]. The fact that the pair is very tightly regulated, and the DraT is highly efficient and specific for the singular target, is reminiscent of the classical bacterial ART toxins. Therefore, DraT/DraG can be considered a “domesticated” TA system [2,176].

The structure for DraT is not available, probably due to its instability *in vitro*. It is known that it requires the presence of another stabilizing/activating protein, a P protein. The activity of DraT is similar to other bacterial toxin ARTs, and due to the conserved R-S-E motif, it belongs to the CTX family [175] (Table 1 and Fig. 2).

#### 5.2. DarT/DarG

TA pair composed of DarT transferase and its cognate hydrolase DarG have been found in, so far, only several various bacteria including pathogens such as *Mycobacterium tuberculosis* and *Klebsiella pneumoniae* and opportunistic pathogen *Pseudomonas mendocina* [177–179]. DarT/DarG is the first characterized system for the reversible ADP-ribosylation of nucleic acids.

DarT is, on its own, better represented in bacterial genomes (0.2% out of 200 000 bacterial genomes). It strictly MARYlates the single-stranded DNA on specific thymidine residues in the TNTC, TTT or TCT motifs. The consequences of DarT MARYlation is impairment of cellular processes essential for bacterial growth and activation of the SOS response. The formation of the ADPr-DNA adduct is reversed via the action of DarG, which shares some functional features with human orthologue TARG1 [179]. In enteropathic *E. coli*, it was also shown that the MARYlated DNA blocks replication as the DNA-ADPr is perceived as DNA damage, suggesting that host bacteria may exploit this system to induce persistence [179–180]. DarG antitoxin activity is indispensable for resuming growth and an essential gene when DarT is present [180–181].

The DarG macrodomain adopts a typical macrodomain fold and is structurally most similar to eukaryotic TARG1. Since these two enzymes share de-MARYlation activity and the overall shape of the macrodomain ligand-binding pocket as well as the ligand position, it was considered that they also share a catalytic activity. The first proposed catalytic mechanism of TARG1 included the nucleophilic attack of Lys84 on the ribose-C1' position and formation of an open ring Amadori product, but further functional analysis of Glu125 which makes catalytic duo with Lys84 [155] led to a proposal of a second catalytic mechanism. Such a mechanism would involve deprotonation of Lys84 by Glu125 and then a nucleophilic attack that leads to the formation of a Schiff base. Further, a nucleophilic attack of a water molecule activated by Glu125 leads to the formation of ring-opened ADPr and enables regeneration of the catalytic lysine [155,179]. DarG contains one of the catalytic duo - residue Lys80 but lacks the glutamate equivalent (Fig. 2). Indeed, the mutation of Lys80 in DarG showed the most significant effect on substrate turnover out of all mutants tested and resulted in inactive DarG indicating the importance of this conserved lysine residue. Still, the complete catalytic mechanism remains elusive.

### 5.3. SirTM

A distinct class of sirtuins, SirTM, are found predominantly in pathogenic bacteria. What clearly distinguishes them from other sirtuins is a very robust ART activity and genetic linkage to a specific subclass of MacroD-like hydrolases, which reverse the sirtuin catalysed ADP-ribosylation [112].

SirTMs in opportunistic pathogens *Staphylococcus aureus* and *Streptococcus pyogenes* were described. The ART and macrodomain hydrolase genes come in an operon with two more genes - modification carrier protein (GcvH-L) and a lipotease. The target protein GcvH-L is modified twice in sequential order - firstly by the lipotease (synthesising protein lipoylation) and then MARYlated by SirTM. The lipoylation is a prerequisite for the ART activity of the SirTM. The key histidine residue and crucial for deacetylase activity in all sirtuins is replaced by Gln137 in SirTMs. Mutation of Gln137 in addition to Asn118 and Arg192 dramatically decreased the catalytic activity, pointing to this as the SirTM catalytic trio (Fig. 3I). The MARYlation can be reversed by sirtuins-dependent MacroD-like hydrolase [112]. They contain an extended catalytic loop containing a zinc-binding motif instead of typical glycine-rich stretch going into  $\alpha$ -helix 6, and an amino acid exchange in the catalytic loop. The Zn<sup>2+</sup> found in the active site suggests it is involved in the catalytic function which would be unique for the members of this class of MacroD-like hydrolases [182].

The system establishes crosstalk between lipoylation and MARYlation and it is possible these PTMs together modulate microbial virulence by regulating the response to host-derived reactive oxygen species. SirTMs can be found in other pathogenic bacteria (Clostridiaceae, Enterococcaceae, Lachnospiraceae, Spirochaetaceae, and Veillonellaceae families) and fungi (Aspergillus,

*Candida*, *Entamoeba*, *Fusarium*, and *Phytophthora* genera etc.) [112].

### 5.4. ParT/ParS

The endotoxin module from *Shingobium* sp. YBL2 ParT/ParS functions as a TA system and is found in 18% of bacterial species. The ParT is an unusually small ART (~18 kDa), which may mean it is evolutionarily old. It contains the RES domain (Table 1), although its typical triad motif R-Y-N differs from both DTX and CTX family (Fig. 2). The alanine scan on the highly conserved residues Arg31, Glu52, and His56 resulted in the elimination of the toxic phenotype, suggesting these to be the catalytic residues (Fig. 3K). ParT specifically MARYlates *E. coli* phosphoribosyl pyrophosphate synthetase (Prs), an essential enzyme in nucleotide biosynthesis conserved among all free-living organisms. Modification sites are Lys182 (located in the ATP-binding site) or Ser202. ParS counteracts the ParT activity through protein interaction inhibition [183].

### 5.5. SidE/SidJ/DupA

A new class of ubiquitin targeting CTX family ARTs has been described. The best-studied example is the human pathogenic bacterium *Legionella pneumophila* proteins, the SidE enzymes (SdeA, SdeB, SdeC and SidE). Their activity can be counteracted at two levels by SidJ, the calmodulin-dependent glutamylase and by DupA and DupB, the two deubiquitinases [184–193]. The SdeA-C, SidJ and the DupA reside within the same operon [192].

The full-length SdeA protein (best described of the SidE-type enzymes) contains four domains: an N-terminal deubiquitinase (DUB) domain, a phosphodiesterase (PDE) domain, a MARYlating ART domain (mART), and a C-terminal putative coiled-coil (CC) domain (Table 1). The mART domain contains the R-S-[EXE] motif with two conserved glutamates (Glu860 and Glu862) as key residues for enzymatic activity (Fig. 2). It transfers ADPr onto Arg42 of ubiquitin (Ub) and the PDE domain cleaves the ADPr-Ub to phosphoribosyl(PR)-Ub which is then conjugated to substrate serines. SidE enzymes target more than 180 different proteins within the infected cells [192]. The most prominent ones are the Rab small GTPases [186,194–195], reticulon-type ER membrane proteins [201], mitochondrial proteins and Golgi components [185,192,194]. The SidJ has been first proposed to act as a deubiquitinase [186], but recent findings indicate that SidJ acts as a glutamylase that inhibits SidE enzymes by targeting the catalytic site of their mART domain [188–190]. The activity of SidJ is essential for its role in *L. pneumophila* infection [186]. The actual reversing of the SidE enzymes activity is performed by DupA and DupB, the deubiquitinases which structurally resemble the PDE domain of SdeA and SidE. DupA/B PDE preference for deubiquitinating activity is governed by their high interaction affinity and longer residence time of the PR-Ub substrate in comparison to that one of SidEs [192].

A similar to SdeA, Ub-specific ART CteC from *Chromobacterium violaceum* specifically MARYlates Thr66 of ubiquitin both in mono- and poly-Ub state, which inhibits poly-Ub chain synthesis. Two homologous proteins, CHBU from *Burkholderia ubonensis* and CHCS from *Coralloccoccus* sp., show 66% and 24% sequence identity with CteC, respectively, and the same activity. All three proteins seem to have the R-S-E motif but otherwise show no predicted structural similarity with the CTX family [196].

### 5.6. Tre1/Tri1

Tre1 (Type IV secretion ART effector 1) from *Serratia proteamaculans* (insect pathogen) is the best-studied member of a small group of bacterial ART which MARYlate several bacterial proteins

and act as an interbacterial defence system. This ART group comes in operons containing an immunoprotein that can neutralize the toxin via interaction and occlusion of the active site or by harbouring an ARH domain. Among the targets are the proteins involved in cell division (tubulin-like FtsZ), translation (EF-Tu), RNA metabolism (RNase E), and lipoprotein transport (LoID). MARYlation of FtsZ by Tre1 was closely examined and it shows modification on Arg174. The modification efficiently abolishes the FtsZ function in Z-ring formation and cell division. Tre1 is a typical R-S-E ART (Fig. 2), as the mutation of the glutamic acid abolishes its activity. Its immunoprotein Tri1 has a two for one mode of protection; it occludes the active site of Tre1 with its N-terminal extension and has a DraG-like domain that reverses Tre1 ART activity (Table 2 and Fig. 2). Upon closer analysis of other DraG-like immunity proteins and their N-terminal extensions, the authors suggest these dual immunity proteins might be quite common, especially among Gram-negative bacteria [197].

## 6. Conclusions

Almost 60 years of research on the ADP-ribosylation system has yielded an enviable amount of knowledge, placing this system right at the core of many essential pathways such as DNA-damage repair, DNA replication, transcription, signal transduction, cell division, stress and infection responses, microbial pathogenicity, and ageing. While the focus was put primarily on the mammalian homologues, the bacterial world of ARTs, sirtuins and ARHs, and more expanded, offering candidates for each type of enzymes found in their evolutionarily higher counterparts, and more. Bacterial and viral versions of ART, sirtuin, Macro, and DraG-like domains in diverse conflict systems offer the potential for understanding the nature of these conflict systems, the true diversity of biochemical activities of the ADP-ribosylation system and the possibility of new solutions to antimicrobial and viral treatments. Despite the accumulated knowledge, one is left wanting more understanding of the molecular mechanisms governing ADP-ribosylation signalling and the physiological and pathophysiological importance of the pathways regulated by ADP-ribosylation. Thus, we can expect much more exciting data to be added to the pool of knowledge, including the current efforts of tackling the search for an inhibitor of the viral macrodomain found in the SARS-CoV-2 to fight the ongoing pandemic [134,142,153,198]. Also, we do know that enzymatic reactions of ADP-ribosylation are central in the pathogenesis of many human diseases and infections. The post-antibiotic era has raised the need to find alternative ways to fight pathogenic bacteria as major ones are becoming resistant to the existing antibiotics. The newly found in-depth understanding of ADP-ribosylation reactions will provide the rationale for designing novel antimicrobial strategies for the treatment of current and future infectious diseases.

## CRediT authorship contribution statement

**Petra Mikolčević:** Conceptualization, Investigation, Data curation, Writing - original draft. **Andrea Hloušek-Kasun:** Conceptualization, Investigation, Data curation, Writing - original draft. **Ivan Ahel:** Funding acquisition, Supervision, Writing - review & editing. **Andreja Mikoč:** Funding acquisition, Supervision, Writing - review & editing

## Declaration of Competing Interest

The authors declare that they have no known competing financial interests or personal relationships that could have appeared to influence the work reported in this paper.

## Acknowledgements

The authors are grateful to Johannes Gregor Matthias Rack (University of Oxford) for the constructive comments on the manuscript. This work is supported by the Croatian Science Foundation (Projects No. IP-2016-06-4242 and IP-CORONA-2020-04-2041). P. M. is supported by Horizon 2020 Widening Fellowship grant (867468 – STREPUNLOCKED). Work in I.A.'s laboratory was supported by Wellcome Trust (101794, 210634); Biotechnology and Biological Sciences Research Council (BB/R007195/1); and Cancer Research United Kingdom (C35050/A22284).

## References

- [1] Kozłowski LP. Proteome-pl: proteome isoelectric point database. *Nucleic Acids Res* 2017;45:D1112–6. <https://doi.org/10.1093/nar/gkw978>.
- [2] Aravind L, Zhang D, de Souza RF, Anand S, Iyer LM. The natural history of ADP-ribosyltransferases and the ADP-ribosylation system. *Curr Top Microbiol Immunol* 2015;384:3–32. [https://doi.org/10.1007/82\\_2014\\_414](https://doi.org/10.1007/82_2014_414).
- [3] Perina D et al. Distribution of protein poly(ADP-ribosylation) systems across all domains of life. *DNA Repair* 2014;23:4–16. <https://doi.org/10.1016/j.dnarep.2014.05.003>.
- [4] Slade D et al. The structure and catalytic mechanism of a poly(ADP-ribose) glycohydrolase. *Nature* 2011;477:616–20. <https://doi.org/10.1038/nature10404>.
- [5] Daugherty MD, Young JM, Kerns JA, Malik HS. Rapid evolution of PARP genes suggests a broad role for ADP-ribosylation in host-virus conflicts. *PLoS Genet* 2014;10: <https://doi.org/10.1371/journal.pgen.1004403> e1004403.
- [6] Cohen MS, Chang P. Insights into the biogenesis, function, and regulation of ADP-ribosylation. *Nat Chem Biol* 2018;14:236–43. <https://doi.org/10.1038/nchembio.2568>.
- [7] Alhammad YMO, Fehr AR. The Viral Macrodomain Counters Host Antiviral ADP-Ribosylation. *Viruses* 2020;12. <https://doi.org/10.3390/v12040384>.
- [8] Catara G, Corteggio A, Valente C, Grimaldi G, Palazzo L. Targeting ADP-ribosylation as an antimicrobial strategy. *Biochem Pharmacol* 2019;167:13–26. <https://doi.org/10.1016/j.bcp.2019.06.001>.
- [9] Huh JW, Shima J, Ochi K. ADP-ribosylation of proteins in *Bacillus subtilis* and its possible importance in sporulation. *J Bacteriol* 1996;178:4935–41. <https://doi.org/10.1128/jb.178.16.4935-4941.1996>.
- [10] Eastman D, Dworkin M. Endogenous ADP-ribosylation during development of the prokaryote *Myxococcus xanthus*. *Microbiology (Reading)* 1994;140(Pt 11):3167–76. <https://doi.org/10.1099/13500872-140-11-3167>.
- [11] Hildebrandt K, Eastman D, Dworkin M. ADP-ribosylation by the extracellular fibrils of *Myxococcus xanthus*. *Mol Microbiol* 1997;23:231–5. <https://doi.org/10.1046/j.1365-2958.1997.2111575.x>.
- [12] Palazzo L, Mikoc A, Ahel I. ADP-ribosylation: new facets of an ancient modification. *FEBS J* 2017;284:2932–46. <https://doi.org/10.1111/febs.14078>.
- [13] Ochi K, Penyige A, Barabas G. The possible role of ADP-ribosylation in sporulation and streptomycin production by *Streptomyces griseus*. *J Gen Microbiol* 1992;138(Pt 8):1745–50. <https://doi.org/10.1099/00221287-138-8-1745>.
- [14] Penyige A, Deak E, Kalmanczhelyi A, Barabas G. Evidence of a role for NAD<sup>+</sup>-glycohydrolase and ADP-ribosyltransferase in growth and differentiation of *Streptomyces griseus* NRRL B-2682: inhibition by m-aminophenylboronic acid. *Microbiology (Reading)* 1996;142(Pt 8):1937–44. <https://doi.org/10.1099/13500872-142-8-1937>.
- [15] Szirak K et al. Disruption of SCO5461 gene coding for a mono-ADP-ribosyltransferase enzyme produces a conditional pleiotropic phenotype affecting morphological differentiation and antibiotic production in *Streptomyces coelicolor*. *J Microbiol* 2012;50:409–18. <https://doi.org/10.1007/s12275-012-1440-y>.
- [16] Penyige A et al. Analysis and identification of ADP-ribosylated proteins of *Streptomyces coelicolor* M145. *J Microbiol* 2009;47:549–56. <https://doi.org/10.1007/s12275-009-0032-y>.
- [17] Bentley SD et al. Complete genome sequence of the model actinomycete *Streptomyces coelicolor* A3(2). *Nature* 2002;417:141–7. <https://doi.org/10.1038/417141a>.
- [18] Penyige A, Barabas G, Szabo I, Ensign JC. ADP-ribosylation of membrane proteins of *Streptomyces griseus* strain 52-1. *FEMS Microbiol Lett* 1990;57:293–7. [https://doi.org/10.1016/0378-1097\(90\)90083-3](https://doi.org/10.1016/0378-1097(90)90083-3).
- [19] Shima J, Penyige A, Ochi K. Changes in patterns of ADP-ribosylated proteins during differentiation of *Streptomyces coelicolor* A3(2) and its development mutants. *J Bacteriol* 1996;178:3785–90. <https://doi.org/10.1128/jb.178.13.3785-3790.1996>.
- [20] Penyige A, Saido-Sakanaka H, Ochi K. Endogenous ADP-Ribosylation of Proteins during Development of *Streptomyces griseus*. *Actinomycetologica* 1996;10:98–103. [https://doi.org/10.3209/saj.10\\_98](https://doi.org/10.3209/saj.10_98).
- [21] Lalic J et al. Disruption of Macrodomain Protein SCO6735 Increases Antibiotic Production in *Streptomyces coelicolor*. *J Biol Chem* 2016;291:23175–87. <https://doi.org/10.1074/jbc.M116.721894>.

- [22] Simon NC, Aktories K, Barbieri JT. Novel bacterial ADP-ribosylating toxins: structure and function. *Nat Rev Microbiol* 2014;12:599–611. <https://doi.org/10.1038/nrmicro3310>.
- [23] Vyas S et al. Family-wide analysis of poly(ADP-ribose) polymerase activity. *Nat Commun* 2014;5:4426. <https://doi.org/10.1038/ncomms5426>.
- [24] Butepage M, Ecker L, Verheugd P, Luscher B. Intracellular Mono-ADP-Ribosylation in Signaling and Disease. *Cells* 2015;4:569–95. <https://doi.org/10.3390/cells4040569>.
- [25] Luscher B et al. ADP-Ribosylation, a Multifaceted Posttranslational Modification Involved in the Control of Cell Physiology in Health and Disease. *Chem Rev* 2018;118:1092–136. <https://doi.org/10.1021/acs.chemrev.7b00122>.
- [26] Rack JGM, Palazzo L, Ahel I. (ADP-ribosyl)hydrolases: structure, function, and biology. *Genes Dev* 2020;34:263–84. <https://doi.org/10.1101/gad.334631.119>.
- [27] Yoshida T, Tsuge H. Common Mechanism for Target Specificity of Protein- and DNA-Targeting ADP-Ribosyltransferases. *Toxins* 2021;13. <https://doi.org/10.3390/toxins13010040>.
- [28] Holbourn KP, Shone CC, Acharya KR. A family of killer toxins. Exploring the mechanism of ADP-ribosylating toxins. *FEBS J* 2006;273:4579–93. <https://doi.org/10.1111/j.1742-4658.2006.05442.x>.
- [29] Hawse WF, Wolberger C. Structure-based mechanism of ADP-ribosylation by sirtuins. *J Biol Chem* 2009;284:33654–61. <https://doi.org/10.1074/jbc.M109.024521>.
- [30] Wilson BA, Reich KA, Weinstein BR, Collier RJ. Active-site mutations of diphtheria toxin: effects of replacing glutamic acid-148 with aspartic acid, glutamine, or serine. *Biochemistry* 1990;29:8643–51. <https://doi.org/10.1021/bi00489a021>.
- [31] Hottiger MO, Hassa PO, Luscher B, Schuler H, Koch-Nolte F. Toward a unified nomenclature for mammalian ADP-ribosyltransferases. *Trends Biochem Sci* 2010;35:208–19. <https://doi.org/10.1016/j.tibs.2009.12.003>.
- [32] Parikh SL, Schramm VL. Transition state structure for ADP-ribosylation of eukaryotic elongation factor 2 catalyzed by diphtheria toxin. *Biochemistry* 2004;43:1204–12. <https://doi.org/10.1021/bi035907z>.
- [33] Quan S et al. ADP-ribosylation as an intermediate step in inactivation of rifampin by a mycobacterial gene. *Antimicrob Agents Chemother* 1999;43:181–4.
- [34] Barkauskaite E, Jankevicius G, Ahel I. Structures and Mechanisms of Enzymes Employed in the Synthesis and Degradation of PARP-Dependent Protein ADP-Ribosylation. *Mol Cell* 2015;58:935–46. <https://doi.org/10.1016/j.molcel.2015.05.007>.
- [35] Bonfiglio, J. J. et al. Serine ADP-Ribosylation Depends on HPF1. *Molecular cell* 65, 932–940 e936, 10.1016/j.molcel.2017.01.003 (2017).
- [36] Buch-Larsen SC et al. Mapping Physiological ADP-Ribosylation Using Activated Ion Electron Transfer Dissociation. *Cell Rep* 2020;32. <https://doi.org/10.1016/j.celrep.2020.108176>.
- [37] Crawford K, Bonfiglio JJ, Mikoc A, Matic I, Ahel I. Specificity of reversible ADP-ribosylation and regulation of cellular processes. *Crit Rev Biochem Mol Biol* 2018;53:64–82. <https://doi.org/10.1080/10409238.2017.1394265>.
- [38] Baysarowich J et al. Rifampicin antibiotic resistance by ADP-ribosylation: Structure and diversity of Arr. *PNAS* 2008;105:4886–91. <https://doi.org/10.1073/pnas.0711939105>.
- [39] Jorgensen R et al. Cholix toxin, a novel ADP-ribosylating factor from *Vibrio cholerae*. *J Biol Chem* 2008;283:10671–8. <https://doi.org/10.1074/jbc.M710008200>.
- [40] Jorgensen R, Wang Y, Visschedyk D, Merrill AR. The nature and character of the transition state for the ADP-ribosyltransferase reaction. *EMBO Rep* 2008;9:802–9. <https://doi.org/10.1038/embor.2008.90>.
- [41] Mansfield MJ, Sugiman-Marangos SN, Melnyk RA, Dooxey AC. Identification of a diphtheria toxin-like gene family beyond the *Corynebacterium* genus. *FEBS Lett* 2018;592:2693–705. <https://doi.org/10.1002/1873-3468.13208>.
- [42] Gillet, D. & Barbier, J. Diphtheria Toxin. The Comprehensive Sourcebook of Bacterial Protein Toxins. 111–132, 10.1016/B978-0-12-800188-2.00004-5; 2015.
- [43] Liu S, Milne GT, Kuremsky JG, Fink GR, Leppla SH. Identification of the proteins required for biosynthesis of diphthamide, the target of bacterial ADP-ribosylating toxins on translation elongation factor 2. *Mol Cell Biol* 2004;24:9487–97. <https://doi.org/10.1128/MCB.24.21.9487-9497.2004>.
- [44] Michalska M, Wolf P. *Pseudomonas* Exotoxin A: optimized by evolution for effective killing. *Front Microbiol* 2015;6:963. <https://doi.org/10.3389/fmicb.2015.00963>.
- [45] Falnes PO, Ariansen S, Sandvig K, Olsnes S. Requirement for prolonged action in the cytosol for optimal protein synthesis inhibition by diphtheria toxin. *J Biol Chem* 2000;275:4363–8. <https://doi.org/10.1074/jbc.275.6.4363>.
- [46] Young JC et al. The *Escherichia coli* effector EspJ blocks Src kinase activity via amidation and ADP ribosylation. *Nat Commun* 2014;5:5887. <https://doi.org/10.1038/ncomms6887>.
- [47] Pollard DJ et al. The Type III Secretion System Effector SeoC of *Salmonella enterica* subsp. *salamae* and *S. enterica* subsp. *arizonae* ADP-Ribosylates Src and Inhibits Opsonophagocytosis. *Infect Immun* 2016;84:3618–28. <https://doi.org/10.1128/IAI.00704-16>.
- [48] Singer AU et al. Crystal structures of the type III effector protein AvrPphF and its chaperone reveal residues required for plant pathogenesis. *Structure* 2004;12:1669–81. <https://doi.org/10.1016/j.str.2004.06.023>.
- [49] Cheng RA, Wiedmann M. The ADP-Ribosylating Toxins of *Salmonella*. *Toxins* 2019;11. <https://doi.org/10.3390/toxins11070416>.
- [50] Garcia-Saura AG, Zapata-Perez R, Hidalgo JF, Sanchez-Ferrer A. Comparative inhibitory profile and distribution of bacterial PARPs, using *Clostridioides difficile* CD160 PARP as a model. *Sci Rep* 2018;8:8056. <https://doi.org/10.1038/s41598-018-26450-0>.
- [51] Cho CC, Chien CY, Chiu YC, Lin MH, Hsu CH. Structural and biochemical evidence supporting poly ADP-ribosylation in the bacterium *Deinococcus radiodurans*. *Nat Commun* 2019;10:1491. <https://doi.org/10.1038/s41467-019-09153-6>.
- [52] Shin JH, Eom H, Song WJ, Rho M. Integrative metagenomic and biochemical studies on rifampicin ADP-ribosyltransferases discovered in the sediment microbiome. *Sci Rep* 2018;8:12143. <https://doi.org/10.1038/s41598-018-30547-x>.
- [53] Stallings CL, Chu L, Li LX, Glickman MS. Catalytic and non-catalytic roles for the mono-ADP-ribosyltransferase Arr in the mycobacterial DNA damage response. *PLoS ONE* 2011;6. <https://doi.org/10.1371/journal.pone.0021807>.
- [54] Agrawal P, Varada R, Sah S, Bhattacharyya S, Varshney U. Species-Specific Interactions of Arr with RplK Mediate Stringent Response in Bacteria. *J Bacteriol* 2018;200. <https://doi.org/10.1128/JB.00722-17>.
- [55] Swaminath, S., Pradhan, A., Nair, R. R. & Ajitkumar, P. The rifampicin-inactivating mono-ADP-ribosyl transferase of *Mycobacterium smegmatis* significantly influences reactive oxygen species levels in the actively growing cells. *bioRxiv* : the preprint server for biology, 2020.2001.2010.902668, 10.1101/2020.01.10.902668 (2020).
- [56] Littler DR et al. Structure-function analyses of a pertussis-like toxin from pathogenic *Escherichia coli* reveal a distinct mechanism of inhibition of trimeric G-proteins. *J Biol Chem* 2017;292:15143–58. <https://doi.org/10.1074/jbc.M117.796094>.
- [57] Martinez M, Price SR, Moss J, Alvarez-Gonzalez R. Mono(ADP-ribosyl)ation of poly(ADP-ribose)polymerase by cholera toxin. *Biochem Biophys Res Commun* 1991;181:1412–8. [https://doi.org/10.1016/0006-291x\(91\)92096-3](https://doi.org/10.1016/0006-291x(91)92096-3).
- [58] Osborne Jr JC, Stanley SJ, Moss J. Kinetic mechanisms of two NAD:arginine ADP-ribosyltransferases: the soluble, salt-stimulated transferase from turkey erythrocytes and cholera toxin, a toxin from *Vibrio cholerae*. *Biochemistry* 1985;24:5235–40. <https://doi.org/10.1021/bi00340a042>.
- [59] Milligan G, Mitchell FM. An arginine residue is the site of receptor-stimulated, cholera toxin-catalysed ADP-ribosylation of pertussis toxin-sensitive G-proteins. *Cell Signal* 1993;5:485–93. [https://doi.org/10.1016/0898-6568\(93\)90088-4](https://doi.org/10.1016/0898-6568(93)90088-4).
- [60] Laing S, Unger M, Koch-Nolte F, Haag F. ADP-ribosylation of arginine. *Amino acids* 2011;41:257–69. <https://doi.org/10.1007/s00726-010-0676-2>.
- [61] Watanabe M et al. Enzymatic properties of pierisin-1 and its N-terminal domain, a guanine-specific ADP-ribosyltransferase from the cabbage butterfly. *J Biochem* 2004;135:471–7. <https://doi.org/10.1093/jb/mvh062>.
- [62] Watanabe M et al. Molecular cloning of an apoptosis-inducing protein, pierisin, from cabbage butterfly: possible involvement of ADP-ribosylation in its activity. *PNAS* 1999;96:10608–13. <https://doi.org/10.1073/pnas.96.19.10608>.
- [63] Nakano T et al. ADP-ribosylation of guanosine by SC05461 protein secreted from *Streptomyces coelicolor*. *Toxin: Off J Int Soc Toxinol* 2013;63:55–63. <https://doi.org/10.1016/j.toxinon.2012.11.019>.
- [64] Nakano T, Takahashi-Nakaguchi A, Yamamoto M, Watanabe M. Pierisins and CARP-1: ADP-ribosylation of DNA by ARTCs in butterflies and shellfish. *Curr Top Microbiol Immunol* 2015;384:127–49. [https://doi.org/10.1007/82\\_2014\\_416](https://doi.org/10.1007/82_2014_416).
- [65] Carpusa I, Jank T, Aktories K. *Bacillus sphaericus* mosquitoicidal toxin (MTX) and pierisin: the enigmatic offspring from the family of ADP-ribosyltransferases. *Mol Microbiol* 2006;62:621–30. <https://doi.org/10.1111/j.1365-2958.2006.05401.x>.
- [66] Duan Q, Xia P, Nandre R, Zhang W, Zhu G. Review of Newly Identified Functions Associated With the Heat-Labile Toxin of Enterotoxigenic *Escherichia coli*. *Front Cell Infect Microbiol* 2019;9:292. <https://doi.org/10.3389/fcimb.2019.00292>.
- [67] Carbonetti NH. Contribution of pertussis toxin to the pathogenesis of pertussis disease. *Pathog Dis* 2015;73:ftv073. <https://doi.org/10.1093/femspd/ftv073>.
- [68] Krueger KM, Barbieri JT. The family of bacterial ADP-ribosylating exotoxins. *Clin Microbiol Rev* 1995;8:34–47.
- [69] Moss J, Vaughan M. Activation of cholera toxin by ADP-ribosylation factors, 20-kDa guanine nucleotide-binding proteins. *Curr Top Cell Regul* 1992;32:49–72. <https://doi.org/10.1016/b978-0-12-152832-4.50004-5>.
- [70] Moss J, Vaughan M. Activation of cholera toxin and *Escherichia coli* heat-labile enterotoxins by ADP-ribosylation factors, a family of 20 kDa guanine nucleotide-binding proteins. *Mol Microbiol* 1991;5:2621–7. <https://doi.org/10.1111/j.1365-2958.1991.tb01971.x>.
- [71] Janicot M, Fouque F, Desbuquois B. Activation of rat liver adenylate cyclase by cholera toxin requires toxin internalization and processing in endosomes. *J Biol Chem* 1991;266:12858–65.
- [72] van den Akker F et al. The Arg7Lys mutant of heat-labile enterotoxin exhibits great flexibility of active site loop 47–56 of the A subunit. *Biochemistry* 1995;34:10996–1004. <https://doi.org/10.1021/bi00035a005>.
- [73] de Souza RF, Aravind L. Identification of novel components of NAD-utilizing metabolic pathways and prediction of their biochemical functions. *Mol Biosyst* 2012;8:1661–77. <https://doi.org/10.1039/c2mb05487f>.
- [74] Cieplak Jr W, Mead DJ, Messer RJ, Grant CC. Site-directed mutagenic alteration of potential active-site residues of the A subunit of *Escherichia*

- coli heat-labile enterotoxin. Evidence for a catalytic role for glutamic acid 112. *J Biol Chem* 1995;270:30545–50. <https://doi.org/10.1074/jbc.270.51.30545>.
- [75] Song J, Gao X, Galan JE. Structure and function of the Salmonella Typhi chimaeric A(2)B(5) typhoid toxin. *Nature* 2013;499:350–4. <https://doi.org/10.1038/nature12377>.
- [76] Tamamura Y, Tanaka K, Uchida I. Characterization of pertussis-like toxin from Salmonella spp. that catalyzes ADP-ribosylation of G proteins. *Sci Rep* 2017;7:2653. <https://doi.org/10.1038/s41598-017-02517-2>.
- [77] Uchida I et al. Salmonella enterica serotype Typhimurium DT104 ArtA-dependent modification of pertussis toxin-sensitive G proteins in the presence of [32P]NAD. *Microbiology (Reading)* 2009;155:3710–8. <https://doi.org/10.1099/mic.0.028399-0>.
- [78] Sakurai J, Nagahama M, Oda M, Tsuge H, Kobayashi K. Clostridium perfringens iota-toxin: structure and function. *Toxins* 2009;1:208–28. <https://doi.org/10.3390/toxins1020208>.
- [79] Visschedyk D et al. Certhax toxin, an anthrax-related ADP-ribosyltransferase from *Bacillus cereus*. *J Biol Chem* 2012;287:41089–102. <https://doi.org/10.1074/jbc.M112.412809>.
- [80] Zhang D, de Souza RF, Anantharaman V, Iyer LM, Aravind L. Polymorphic toxin systems: Comprehensive characterization of trafficking modes, processing, mechanisms of action, immunity and ecology using comparative genomics. *Biology direct* 2012;7:18. <https://doi.org/10.1186/1745-6150-7-18>.
- [81] Evans HR et al. The crystal structure of C3stau2 from *Staphylococcus aureus* and its complex with NAD. *J Biol Chem* 2003;278:45924–30. <https://doi.org/10.1074/jbc.M307719200>.
- [82] Aktories K, Braun U, Rosener S, Just I, Hall A. The rho gene product expressed in *E. coli* is a substrate of botulinum ADP-ribosyltransferase C3. *Biochem Biophys Res Commun* 1989;158:209–13. [https://doi.org/10.1016/s0006-291x\(89\)80199-8](https://doi.org/10.1016/s0006-291x(89)80199-8).
- [83] Barbieri JT, Sun J. *Pseudomonas aeruginosa* ExoS and ExoT. *Rev Physiol Biochem Pharmacol* 2004;152:79–92. <https://doi.org/10.1007/s10254-004-0031-7>.
- [84] Reinert DJ, Carpusca I, Aktories K, Schulz GE. Structure of the mosquitocidal toxin from *Bacillus sphaericus*. *J Mol Biol* 2006;357:1226–36. <https://doi.org/10.1016/j.jmb.2006.01.025>.
- [85] Oda T et al. Structural basis of autoinhibition and activation of the DNA-targeting ADP-ribosyltransferase pierisin-1. *J Biol Chem* 2017;292:15445–55. <https://doi.org/10.1074/jbc.M117.776641>.
- [86] Lyons B et al. Scabin, a Novel DNA-acting ADP-ribosyltransferase from *Streptomyces scabies*. *J Biol Chem* 2016;291:11198–215. <https://doi.org/10.1074/jbc.M115.707653>.
- [87] Lyons B, Lugo MR, Carlin S, Lidster T, Merrill AR. Characterization of the catalytic signature of Scabin toxin, a DNA-targeting ADP-ribosyltransferase. *Biochem J* 2018;475:225–45. <https://doi.org/10.1042/BCJ20170818>.
- [88] Han S, Tainer JA. The ARTT motif and a unified structural understanding of substrate recognition in ADP-ribosylating bacterial toxins and eukaryotic ADP-ribosyltransferases. *Int J Med Microbiol IJMM* 2002;291:523–9. <https://doi.org/10.1078/1438-4221-00162>.
- [89] Yoshida T, Tsuge H. Substrate N(2) atom recognition mechanism in pierisin family DNA-targeting, guanine-specific ADP-ribosyltransferase ScARP. *J Biol Chem* 2018;293:13768–74. <https://doi.org/10.1074/jbc.AC118.004412>.
- [90] Schirmer J, Wieden HJ, Rodnina MV, Aktories K. Inactivation of the elongation factor Tu by mosquitocidal toxin-catalyzed mono-ADP-ribosylation. *Appl Environ Microbiol* 2002;68:4894–9. <https://doi.org/10.1128/aem.68.10.4894-4899.2002>.
- [91] Depping R, Lohaus C, Meyer HE, Ruger W. The mono-ADP-ribosyltransferases Alt and ModB of bacteriophage T4: target proteins identified. *Biochem Biophys Res Commun* 2005;335:1217–23. <https://doi.org/10.1016/j.bbr.2005.08.023>.
- [92] Alawneh AM, Qi D, Yonesaki T, Otsuka Y. An ADP-ribosyltransferase Alt of bacteriophage T4 negatively regulates the *Escherichia coli* MazF toxin of a toxin-antitoxin module. *Mol Microbiol* 2016;99:188–98. <https://doi.org/10.1111/mmi.13225>.
- [93] Tiemann B et al. ModA and ModB, two ADP-ribosyltransferases encoded by bacteriophage T4: catalytic properties and mutation analysis. *J Bacteriol* 2004;186:7262–72. <https://doi.org/10.1128/JB.186.21.7262-7272.2004>.
- [94] Uzan M, Miller ES. Post-transcriptional control by bacteriophage T4: mRNA decay and inhibition of translation initiation. *Virology journal* 2010;7:360. <https://doi.org/10.1186/1743-422X-7-360>.
- [95] Niu, Y. et al. A Type I-F Anti-CRISPR Protein Inhibits the CRISPR-Cas Surveillance Complex by ADP-Ribosylation. *Molecular cell* 80, 512–524 e515, 10.1016/j.molcel.2020.09.015 (2020).
- [96] Yang S et al. The function of KptA/Tpt1 gene - a minor review. *Funct Plant Biol* : FPB 2020;47:577–91. <https://doi.org/10.1071/FP19159>.
- [97] Spinelli SL, Kierzek R, Turner DH, Phizicky EM. Transient ADP-ribosylation of a 2'-phosphate implicated in its removal from ligated tRNA during splicing in yeast. *J Biol Chem* 1999;274:2637–44. <https://doi.org/10.1074/jbc.274.5.2637>.
- [98] Munnur D et al. Reversible ADP-ribosylation of RNA. *Nucleic Acids Res* 2019;47:5658–69. <https://doi.org/10.1093/nar/gkz2305>.
- [99] Munir A, Banerjee A, Shuman S. NAD<sup>+</sup>-dependent synthesis of a 5'-phospho-ADP-ribosylated RNA/DNA cap by RNA 2'-phosphotransferase Tpt1. *Nucleic Acids Res* 2018;46:9617–24. <https://doi.org/10.1093/nar/gky792>.
- [100] Spinelli SL, Malik HS, Consaul SA, Phizicky EM. A functional homolog of a yeast tRNA splicing enzyme is conserved in higher eukaryotes and in *Escherichia coli*. *PNAS* 1998;95:14136–41. <https://doi.org/10.1073/pnas.95.24.14136>.
- [101] Harding HP et al. An intact unfolded protein response in Trp1 knockout mice reveals phylogenetic divergence in pathways for RNA ligation. *RNA* 2008;14:225–32. <https://doi.org/10.1261/rna.859908>.
- [102] Gajiwala KS, Burley SK. Winged helix proteins. *Curr Opin Struct Biol* 2000;10:110–6. [https://doi.org/10.1016/s0959-440x\(99\)00057-3](https://doi.org/10.1016/s0959-440x(99)00057-3).
- [103] Banerjee A et al. Structure of tRNA splicing enzyme Tpt1 illuminates the mechanism of RNA 2'-PO4 recognition and ADP-ribosylation. *Nat Commun* 2019;10:218. <https://doi.org/10.1038/s41467-018-08211-9>.
- [104] Munir A, Abdullahu L, Damha MJ, Shuman S. Two-step mechanism and step-arrest mutants of *Runella slithyformis* NAD<sup>+</sup>-dependent tRNA 2'-phosphotransferase Tpt1. *RNA* 2018;24:1144–57. <https://doi.org/10.1261/rna.067165.118>.
- [105] Steiger MA, Kierzek R, Turner DH, Phizicky EM. Substrate recognition by a yeast 2'-phosphotransferase involved in tRNA splicing and by its *Escherichia coli* homolog. *Biochemistry* 2001;40:14098–105. <https://doi.org/10.1021/bi011388t>.
- [106] Aravind L. Guilt by association: contextual information in genome analysis. *Genome Res* 2000;10:1074–7. <https://doi.org/10.1101/gr.10.8.1074>.
- [107] Bettini PP et al. *Agrobacterium rhizogenes* rolB gene affects photosynthesis and chlorophyll content in transgenic tomato (*Solanum lycopersicum* L.) plants. *J Plant Physiol* 2016;204:27–35. <https://doi.org/10.1016/j.jplph.2016.07.010>.
- [108] Wang M et al. Molecular insights into plant cell proliferation disturbance by *Agrobacterium* protein 6b. *Genes Dev* 2011;25:64–76. <https://doi.org/10.1101/gad.1985511>.
- [109] Tanny JC, Dowd GJ, Huang J, Hilz H, Moazed D. An enzymatic activity in the yeast Sir2 protein that is essential for gene silencing. *Cell* 1999;99:735–45. [https://doi.org/10.1016/s0092-8674\(00\)81671-2](https://doi.org/10.1016/s0092-8674(00)81671-2).
- [110] Houtkooper RH, Pirinen E, Auwerx J. Sirtuins as regulators of metabolism and healthspan. *Nat Rev Mol Cell Biol* 2012;13:225–38. <https://doi.org/10.1038/nrm3293>.
- [111] Teixeira CSS, Cerqueira N, Gomes P, Sousa SF. A Molecular Perspective on Sirtuin Activity. *Int J Mol Sci* 2020;21. <https://doi.org/10.3390/ijms21228609>.
- [112] Rack JG et al. Identification of a Class of Protein ADP-Ribosylating Sirtuins in Microbial Pathogens. *Mol Cell* 2015;59:309–20. <https://doi.org/10.1016/j.molcel.2015.06.013>.
- [113] Zhao K, Chai X, Marmorstein R. Structure and substrate binding properties of cobB, a Sir2 homolog protein deacetylase from *Escherichia coli*. *J Mol Biol* 2004;337:731–41. <https://doi.org/10.1016/j.jmb.2004.01.060>.
- [114] Sauve AA. Sirtuin chemical mechanisms. *BBA* 1804;1591–1603:2010. <https://doi.org/10.1016/j.bbaap.2010.01.021>.
- [115] Tan Y et al. A SIRT4-like auto ADP-ribosyltransferase is essential for the environmental growth of *Mycobacterium smegmatis*. *Acta Biochim Biophys Sin* 2016;48:145–52. <https://doi.org/10.1093/abbs/gmv121>.
- [116] Xu Q et al. Crystal structure of an ADP-ribosylated protein with a cytidine deaminase-like fold, but unknown function (TM1506), from *Thermotoga maritima* at 2.70 Å resolution. *Proteins* 2008;71:1546–52. <https://doi.org/10.1002/prot.21992>.
- [117] Hoff KG, Avalos JL, Sens K, Wolberger C. Insights into the sirtuin mechanism from ternary complexes containing NAD<sup>+</sup> and acetylated peptide. *Structure* 2006;14:1231–40. <https://doi.org/10.1016/j.str.2006.06.006>.
- [118] Palazzo L et al. Processing of protein ADP-ribosylation by Nudix hydrolases. *Biochem J* 2015;468:293–301. <https://doi.org/10.1042/BJ20141554>.
- [119] Palazzo L et al. ENPP1 processes protein ADP-ribosylation in vitro. *FEBS J* 2016;283:3371–88. <https://doi.org/10.1111/febs.13811>.
- [120] Rack JG, Perina D, Ahel I. Macrod domains: Structure, Function, Evolution, and Catalytic Activities. *Annu Rev Biochem* 2016;85:431–54. <https://doi.org/10.1146/annurev-biochem-060815-014935>.
- [121] Rack J. G. M. et al. (ADP-ribosyl)hydrolases: Structural Basis for Differential Substrate Recognition and Inhibition. *Cell Chem Biol* 25, 1533–1546 e1512, 10.1016/j.chembiol.2018.11.001 (2018).
- [122] Ono T, Kasamatsu A, Oka S, Moss J. The 39-kDa poly(ADP-ribose) glycohydrolase ARH3 hydrolyzes O-acetyl-ADP-ribose, a product of the Sir2 family of acetyl-histone deacetylases. *PNAS* 2006;103:16687–91. <https://doi.org/10.1073/pnas.0607911103>.
- [123] Mueller-Dieckmann C et al. The structure of human ADP-ribosylhydrolase 3 (ARH3) provides insights into the reversibility of protein ADP-ribosylation. *PNAS* 2006;103:15026–31. <https://doi.org/10.1073/pnas.0606762103>.
- [124] Palazzo L et al. Serine is the major residue for ADP-ribosylation upon DNA damage. *Elife* 2018;7. <https://doi.org/10.7554/elife.34334>.
- [125] Mortusewicz O, Fouquerel E, Ame JC, Leonhardt H, Schreiber V. PARC is recruited to DNA damage sites through poly(ADP-ribose)- and PCNA-dependent mechanisms. *Nucleic Acids Res* 2011;39:5045–56. <https://doi.org/10.1093/nar/gkr099>.
- [126] Min W, Cortes U, Herczeg Z, Tong WM, Wang ZQ. Deletion of the nuclear isoform of poly(ADP-ribose) glycohydrolase (PARC) reveals its function in DNA repair, genomic stability and tumorigenesis. *Carcinogenesis* 2010;31:2058–65. <https://doi.org/10.1093/carcin/bqg205>.
- [127] Yang X et al. Molecular basis for the MacroD1-mediated hydrolysis of ADP-ribosylation. *DNA Repair* 2020;94. <https://doi.org/10.1016/j.dnarep.2020.102899>.

- [128] Zapata-Perez R et al. Structural and functional analysis of *Oceanobacillus thelyensis* macrodomain reveals a network of waters involved in substrate binding and catalysis. *Open Biol* 2017;7. <https://doi.org/10.1098/rsob.160327>.
- [129] Chen D et al. Identification of macrodomain proteins as novel O-acetyl-ADP-ribose deacetylases. *J Biol Chem* 2011;286:13261–71. <https://doi.org/10.1074/jbc.M110.206771>.
- [130] Zhang W et al. Structural insights into the mechanism of *Escherichia coli* YmdB: A 2'-O-acetyl-ADP-ribose deacetylase. *J Struct Biol* 2015;192:478–86. <https://doi.org/10.1016/j.jmb.2015.10.010>.
- [131] Hirsch BM, Burgos ES, Schramm VL. Transition-state analysis of 2-O-acetyl-ADP-ribose hydrolysis by human macrodomain 1. *ACS Chem Biol* 2014;9:2255–62. <https://doi.org/10.1021/cb500485w>.
- [132] Jankevicius G et al. A family of macrodomain proteins reverses cellular mono-ADP-ribosylation. *Nat Struct Mol Biol* 2013;20:508–14. <https://doi.org/10.1038/nsmb.2523>.
- [133] Li C et al. Viral Macro Domains Reverse Protein ADP-Ribosylation. *J Virol* 2016;90:8478–86. <https://doi.org/10.1128/JVI.00705-16>.
- [134] Rack JGM et al. Viral macrodomains: a structural and evolutionary assessment of the pharmacological potential. *Open biology* 2020;10. <https://doi.org/10.1098/rsob.200237>.
- [135] Kim KS, Manasherob R, Cohen SN. YmdB: a stress-responsive ribonuclease-binding regulator of *E. coli* RNase III activity. *Genes Dev* 2008;22:3497–508. <https://doi.org/10.1101/gad.1729508>.
- [136] Kim M, Kim M, Kim KS. YmdB-mediated down-regulation of *sucA* inhibits biofilm formation and induces apramycin susceptibility in *Escherichia coli*. *Biochem Biophys Res Commun* 2017;483:252–7. <https://doi.org/10.1016/j.bbr.2016.12.157>.
- [137] Kim T, Lee J, Kim KS. *Escherichia coli* YmdB regulates biofilm formation independently of its role as an RNase III modulator. *BMC Microbiol* 2013;13:266. <https://doi.org/10.1186/1471-2180-13-266>.
- [138] Agnew T et al. MacroD1 Is a Promiscuous ADP-Ribosyl Hydrolase Localized to Mitochondria. *Front Microbiol* 2018;9:20. <https://doi.org/10.3389/fmicb.2018.00020>.
- [139] Grunewald ME et al. The coronavirus macrodomain is required to prevent PARP-mediated inhibition of virus replication and enhancement of IFN expression. *PLoS Pathog* 2019;15. <https://doi.org/10.1371/journal.ppat.1007756>.
- [140] Ferreira-Ramos AS, Sulzenbacher G, Canard B, Coutard B. Snapshots of ADP-ribose bound to Getah virus macro domain reveal an intriguing choreography. *Sci Rep* 2020;10:14422. <https://doi.org/10.1038/s41598-020-70870-w>.
- [141] Cao D, Meng XJ. Molecular biology and replication of hepatitis E virus. *Emerging Microbes Infect* 2012;1. <https://doi.org/10.1038/emi.2012.7e17>.
- [142] Fehr AR, Jankevicius G, Ahel I, Perlman S. Viral Macrodomains: Unique Mediators of Viral Replication and Pathogenesis. *Trends Microbiol* 2018;26:598–610. <https://doi.org/10.1016/j.tim.2017.11.011>.
- [143] Egloff MP et al. Structural and functional basis for ADP-ribose and poly(ADP-ribose) binding by viral macro domains. *J Virol* 2006;80:8493–502. <https://doi.org/10.1128/JVI.00713-06>.
- [144] Malet H et al. The crystal structures of Chikungunya and Venezuelan equine encephalitis virus nsP3 macro domains define a conserved adenosine binding pocket. *J Virol* 2009;83:6534–45. <https://doi.org/10.1128/JVI.00189-09>.
- [145] Chatterjee A et al. Nuclear magnetic resonance structure shows that the severe acute respiratory syndrome coronavirus-unique domain contains a macrodomain fold. *J Virol* 2009;83:1823–36. <https://doi.org/10.1128/JVI.01781-08>.
- [146] Fehr, A. R. et al. The Conserved Coronavirus Macrodomain Promotes Virulence and Suppresses the Innate Immune Response during Severe Acute Respiratory Syndrome Coronavirus Infection. *mBio* 7, 10.1128/mBio.01721-16 (2016).
- [147] Eriksson KK, Cervantes-Barragan L, Ludewig B, Thiel V. Mouse hepatitis virus liver pathology is dependent on ADP-ribose-1"-phosphatase, a viral function conserved in the alpha-like supergroup. *J Virol* 2008;82:12325–34. <https://doi.org/10.1128/JVI.02082-08>.
- [148] Fehr AR et al. The nsp3 macrodomain promotes virulence in mice with coronavirus-induced encephalitis. *J Virol* 2015;89:1523–36. <https://doi.org/10.1128/JVI.02596-14>.
- [149] McPherson RL et al. ADP-ribosylhydrolase activity of Chikungunya virus macrodomain is critical for virus replication and virulence. *PNAS* 2017;114:1666–71. <https://doi.org/10.1073/pnas.1621485114>.
- [150] Lei J, Kusov Y, Hilgenfeld R. Nsp3 of coronaviruses: Structures and functions of a large multi-domain protein. *Antiviral Res* 2018;149:58–74. <https://doi.org/10.1016/j.antiviral.2017.11.001>.
- [151] Frick DN, Virdi RS, Vuksanovic N, Dahal N, Silvaggi NR. Molecular Basis for ADP-Ribose Binding to the Mac1 Domain of SARS-CoV-2 nsp3. *Biochemistry* 2020;59:2608–15. <https://doi.org/10.1021/acs.biochem.0c00309>.
- [152] Babar Z et al. Drug similarity and structure-based screening of medicinal compounds to target macrodomain-I from SARS-CoV-2 to rescue the host immune system: a molecular dynamics study. *J Biomol Struct Dyn* 2020;1–15. <https://doi.org/10.1080/07391102.2020.1815583>.
- [153] Schuller M et al. Fragment Binding to the Nsp3 Macrodomain of SARS-CoV-2 Identified Through Crystallographic Screening and Computational Docking. In: *bioRxiv* : the preprint server for biology. <https://doi.org/10.1101/2020.11.24.393405>.
- [154] Garcia-Saura AG et al. An uncharacterized FMAG\_01619 protein from *Fusobacterium mortiferum* ATCC 9817 demonstrates that some bacterial macrodomains can also act as poly-ADP-ribosylhydrolases. *Sci Rep* 2019;9:3230. <https://doi.org/10.1038/s41598-019-39691-4>.
- [155] Sharifi R et al. Deficiency of terminal ADP-ribose protein glycohydrolase TARG1/C6orf130 in neurodegenerative disease. *EMBO J* 2013;32:1225–37. <https://doi.org/10.1038/emboj.2013.51>.
- [156] Peterson FC et al. Orphan macrodomain protein (human C6orf130) is an O-acetyl-ADP-ribose deacetylase: solution structure and catalytic properties. *J Biol Chem* 2011;286:35955–65. <https://doi.org/10.1074/jbc.M111.276238>.
- [157] Ahel I, Vujaklija D, Mikoc A, Gamulin V. Transcriptional analysis of the *recA* gene in *Streptomyces rimosus*: identification of the new type of promoter. *FEMS Microbiol Lett* 2002;209:133–7. <https://doi.org/10.1111/j.1574-6968.2002.tb11121.x>.
- [158] Gamulin V, Cetkovic H, Ahel I. Identification of a promoter motif regulating the major DNA damage response mechanism of *Mycobacterium tuberculosis*. *FEMS Microbiol Lett* 2004;238:57–63. <https://doi.org/10.1016/j.femsle.2004.07.017>.
- [159] Patel CN, Koh DW, Jacobson MK, Oliveira MA. Identification of three critical acidic residues of poly(ADP-ribose) glycohydrolase involved in catalysis: determining the PARG catalytic domain. *Biochem J* 2005;388:493–500. <https://doi.org/10.1042/BJ20040942>.
- [160] Lambrecht MJ et al. Synthesis of dimeric ADP-ribose and its structure with human poly(ADP-ribose) glycohydrolase. *J Am Chem Soc* 2015;137:3558–64. <https://doi.org/10.1021/ja512528p>.
- [161] Barkauskaite E et al. Visualization of poly(ADP-ribose) bound to PARG reveals inherent balance between exo- and endo-glycohydrolase activities. *Nat Commun* 2013;4:2164. <https://doi.org/10.1038/ncomms3164>.
- [162] Dunstan MS et al. Structure and mechanism of a canonical poly(ADP-ribose) glycohydrolase. *Nat Commun* 2012;3:878. <https://doi.org/10.1038/ncomms1889>.
- [163] Liu Y et al. Transcriptome dynamics of *Deinococcus radiodurans* recovering from ionizing radiation. *PNAS* 2003;100:4191–6. <https://doi.org/10.1073/pnas.0630387100>.
- [164] Jurkevitch, E. Predatory Behaviors in Bacteria – Diversity and Transitions. *Microbe Magazine*, 10.1128/microbe.2.67.1.
- [165] Quinn GR, Skerman VBD. Herpetosiphon—Nature's scavenger?. *Curr Microbiol* 1980;4:57–62. <https://doi.org/10.1007/BF02602893>.
- [166] Li XD et al. Crystal structure of dinitrogenase reductase-activating glycohydrolase (DraG) reveals conservation in the ADP-ribosylhydrolase fold and specific features in the ADP-ribose-binding pocket. *J Mol Biol* 2009;390:737–46. <https://doi.org/10.1016/j.jmb.2009.05.031>.
- [167] Mashimo M, Kato J, Moss J. Structure and function of the ARH family of ADP-ribosyl-acceptor hydrolases. *DNA Repair* 2014;23:88–94. <https://doi.org/10.1016/j.dnarep.2014.03.005>.
- [168] Fontana P et al. Serine ADP-ribosylation reversal by the hydrolase ARH3. *Elife* 2017;6. <https://doi.org/10.7554/eLife.28533>.
- [169] Moss J, Oppenheimer NJ, West Jr RE, Stanley SJ. Amino acid specific ADP-ribosylation: substrate specificity of an ADP-ribosylarginine hydrolase from turkey erythrocytes. *Biochemistry* 1986;25:5408–14. <https://doi.org/10.1021/bi00367a010>.
- [170] Rajendran C et al. Crystal structure of the GlnZ-DraG complex reveals a different form of PII-target interaction. *PNAS* 2011;108:18972–6. <https://doi.org/10.1073/pnas.1108038108>.
- [171] Berthold CL, Wang H, Nordlund S, Hogbom M. Mechanism of ADP-ribosylation removal revealed by the structure and ligand complexes of the dimanganase mono-ADP-ribosylhydrolase DraG. *PNAS* 2009;106:14247–52. <https://doi.org/10.1073/pnas.0905906106>.
- [172] Moure VR et al. Regulation of nitrogenase by reversible mono-ADP-ribosylation. *Curr Top Microbiol Immunol* 2015;384:89–106. [https://doi.org/10.1007/82\\_2014\\_380](https://doi.org/10.1007/82_2014_380).
- [173] Ma Y, Ludden PW. Role of the dinitrogenase reductase arginine 101 residue in dinitrogenase reductase ADP-ribosyltransferase binding, NAD binding, and cleavage. *J Bacteriol* 2001;183:250–6. <https://doi.org/10.1128/JB.183.1.250-256.2001>.
- [174] Wang H, Waluk D, Dixon R, Nordlund S, Noren A. Energy shifts induce membrane sequestration of DraG in *Rhodospirillum rubrum* independent of the ammonium transporters and diazotrophic conditions. *FEMS Microbiol Lett* 2018;365. <https://doi.org/10.1093/femsle/fny176>.
- [175] Nordlund S, Hogbom M. ADP-ribosylation, a mechanism regulating nitrogenase activity. *FEBS J* 2013;280:3484–90. <https://doi.org/10.1111/febs.12279>.
- [176] Ludden PW. Reversible ADP-ribosylation as a mechanism of enzyme regulation in prokaryotes. *Mol Cell Biochem* 1994;138:123–9. <https://doi.org/10.1007/BF00928453>.
- [177] Sberro H et al. Discovery of functional toxin/antitoxin systems in bacteria by shotgun cloning. *Mol Cell* 2013;50:136–48. <https://doi.org/10.1016/j.molcel.2013.02.002>.
- [178] Yamaguchi Y, Park JH, Inouye M. Toxin-antitoxin systems in bacteria and archaea. *Annu Rev Genet* 2011;45:61–79. <https://doi.org/10.1146/annurev-genet-110410-132412>.
- [179] Jankevicius G, Ariza A, Ahel M, Ahel I. The Toxin-Antitoxin System DarTG Catalyzes Reversible ADP-Ribosylation of DNA. *Mol Cell* 2016;64:1109–16. <https://doi.org/10.1016/j.molcel.2016.11.014>.
- [180] Lawaree, E. et al. DNA ADP-Ribosylation Stalls Replication and Is Reversed by RecF-Mediated Homologous Recombination and Nucleotide Excision

- Repair. *Cell Reports* 30, 1373–1384 e1374. Doi: 10.1016/j.celrep.2020.01.014; 2020.
- [181] Zaveri A et al. Depletion of the DarG antitoxin in *Mycobacterium tuberculosis* triggers the DNA-damage response and leads to cell death. *Mol Microbiol* 2020;114:641–52. <https://doi.org/10.1111/mmi.14571>.
- [182] Appel CD, Feld GK, Wallace BD, Williams RS. Structure of the sirtuin-linked macrodomain SAV0325 from *Staphylococcus aureus*. *Protein Sci Publicat Protein Soc* 2016;25:1682–91. <https://doi.org/10.1002/pro.2974>.
- [183] Piscotta FJ, Jeffrey PD, Link AJ. ParST is a widespread toxin-antitoxin module that targets nucleotide metabolism. *PNAS* 2019;116:826–34. <https://doi.org/10.1073/pnas.1814633116>.
- [184] Bhogaraju, S. et al. Phosphoribosylation of Ubiquitin Promotes Serine Ubiquitination and Impairs Conventional Ubiquitination. *Cell* 167, 1636–1649 e1613, 10.1016/j.cell.2016.11.019; 2016.
- [185] Qiu J et al. Ubiquitination independent of E1 and E2 enzymes by bacterial effectors. *Nature* 2016;533:120–4. <https://doi.org/10.1038/nature17657>.
- [186] Qiu J et al. A unique deubiquitinase that deconjugates phosphoribosyl-linked protein ubiquitination. *Cell Res* 2017;27:865–81. <https://doi.org/10.1038/cr.2017.66>.
- [187] Kalayil S et al. Insights into catalysis and function of phosphoribosyl-linked serine ubiquitination. *Nature* 2018;557:734–8. <https://doi.org/10.1038/s41586-018-0145-8>.
- [188] Bhogaraju S et al. Inhibition of bacterial ubiquitin ligases by SidJ-calmodulin catalysed glutamylation. *Nature* 2019;572:382–6. <https://doi.org/10.1038/s41586-019-1440-8>.
- [189] Black MH et al. Bacterial pseudokinase catalyzes protein polyglutamylation to inhibit the SidE-family ubiquitin ligases. *Science* 2019;364:787–92. <https://doi.org/10.1126/science.aaw7446>.
- [190] Gan N et al. Regulation of phosphoribosyl ubiquitination by a calmodulin-dependent glutamylase. *Nature* 2019;572:387–91. <https://doi.org/10.1038/s41586-019-1439-1>.
- [191] Puvar K, Luo ZQ, Das C. Uncovering the Structural Basis of a New Twist in Protein Ubiquitination. *Trends Biochem Sci* 2019;44:467–77. <https://doi.org/10.1016/j.tibs.2018.11.006>.
- [192] Shin, D. et al. Regulation of Phosphoribosyl-Linked Serine Ubiquitination by Deubiquitinases DupA and DupB. *Molecular cell* 77, 164–179 e166, 10.1016/j.molcel.2019.10.019 (2020).
- [193] Sulpizio A et al. Protein polyglutamylation catalyzed by the bacterial calmodulin-dependent pseudokinase SidJ. *Elife* 2019;8. <https://doi.org/10.7554/elife.51162>.
- [194] Kim L et al. Structural and Biochemical Study of the Mono-ADP-Ribosyltransferase Domain of SdeA, a Ubiquitylating/Deubiquitylating Enzyme from *Legionella pneumophila*. *J Mol Biol* 2018;430:2843–56. <https://doi.org/10.1016/j.jmb.2018.05.043>.
- [195] Akturk A et al. Mechanism of phosphoribosyl-ubiquitination mediated by a single *Legionella* effector. *Nature* 2018;557:729–33. <https://doi.org/10.1038/s41586-018-0147-6>.
- [196] Yan, F. et al. Threonine ADP-Ribosylation of Ubiquitin by a Bacterial Effector Family Blocks Host Ubiquitination. *Molecular cell* 78, 641–652 e649, 10.1016/j.molcel.2020.03.016; 2020.
- [197] Ting, S. Y. et al. Bifunctional Immunity Proteins Protect Bacteria against FtsZ-Targeting ADP-Ribosylating Toxins. *Cell* 175, 1380–1392 e1314, 10.1016/j.cell.2018.09.037; 2018.
- [198] Alhammad YMO et al. The SARS-CoV-2 Conserved Macrodomain Is a Mono-ADP-Ribosylhydrolase. *J Virol* 2021;95. <https://doi.org/10.1128/JVI.01969-20>.
- [199] Lugo MR, Lyons B, Lento C, Wilson DJ, Merrill AR. Dynamics of Scabin toxin. A proposal for the binding mode of the DNA substrate. *PLoS ONE* 2018;13:. <https://doi.org/10.1371/journal.pone.0194425>e0194425.
- [200] Treiber N, Reinert DJ, Carpusca I, Aktories K, Schulz GE. Structure and mode of action of a mosquitocidal holotoxin. *J Mol Biol* 2008;381:150–9. <https://doi.org/10.1016/j.jmb.2008.05.067>.
- [201] Kotewicz KM et al. A Single *Legionella* Effector Catalyzes a Multistep Ubiquitination Pathway to Rearrange Tubular Endoplasmic Reticulum for Replication. *Cell Host Microbe* 2017;21:169–81. <https://doi.org/10.1016/j.chom.2016.12.007>.